ADVANCING ANALYTICAL STRATEGIES FOR STEREOISOMER SEPARATION AND GLYCAN CHARACTERIZATION: A HILIC-IM-MS APPROACH

by

MYA BROWN

(Under the Direction of RON ORLANDO)

ABSTRACT

Advancing the separation of isomeric species remains a central challenge in analytical chemistry, particularly for biomolecules like carbohydrates and amino acids where stereochemistry can significantly impact biological function. This dissertation explores strategies that leverage hydrophilic interaction liquid chromatography coupled with ion mobility–mass spectrometry (HILIC-IM-MS) to improve the resolution of stereoisomers and enhance structural glycan characterization.

In the first part, I focused on separating D- and L-monosaccharide isomers using chiral derivatization via reductive amination with amino acids. Tyrosine tagging, in particular, enabled clear ion mobility separation between enantiomers and epimers, revealing how structural variation near the derivatization site affects gas-phase resolution. I then applied a complementary approach to amino acids, derivatizing them with various carbohydrate tags—including mono- and trisaccharides—to improve IM-MS separation. The maltotriose tag proved most effective for resolving 14 out of 17 amino acid enantiomeric pairs and was also extended to peptides containing site-specific D-amino acid substitutions.

The second part of this work focused on improving structural elucidation of N-linked glycans using HILIC retention time modeling. I developed a linear regression model based on monosaccharide retention motifs, creating a retention time prediction tool applicable across neutral and zwitterionic HILIC stationary phases. The model demonstrated strong predictive power, even across changes in column chemistry and gradient conditions, offering a scalable framework for characterizing unknown glycans without relying solely on reference libraries.

Finally, I evaluated mass transfer resistance in HILIC using columns with different pore sizes and particle types. Using dextran ladders, I compared separation efficiency across fully and superficially porous particles and demonstrated that the 160 Å superficially porous column offered the best balance of resolution and band broadening. These results reinforced the importance of column design and the role of the water-enriched stationary phase in HILIC retention mechanisms.

Collectively, these studies present new analytical strategies that improve isomer separation and glycan characterization, providing useful tools for glycomics, metabolomics, and protein chemistry applications.

INDEX WORDS: Ion Mobility, Hydrophobic Interaction Liquid Chromatography, Mass Spectrometry, Glycomics, Retention Prediction

ADVANCING ANALYTICAL STRATEGIES FOR STEREOISOMER SEPARATION AND GLYCAN CHARACTERIZATION: A HILIC-IM-MS APPROACH

by

MYA BROWN

BA, San Diego State University, 2017

MS, Texas Southern University, 2019

A Dissertation Submitted to the Graduate Faculty of The University of Georgia in Partial Fulfillment of the Requirements for the Degree

DOCTOR OF PHILOSOPHY

ATHENS, GEORGIA

2025

ADVANCING ANALYTICAL STRATEGIES FOR STEREOISOMER SEPARATION AND GLYCAN CHARACTERIZATION: A HILIC-IM-MS APPROACH

by

MYA BROWN

Major Professor:	Ron Orlando
Committee:	Jon Amster
	Jeffrey Urbauer

Electronic Version Approved:

Ron Walcott
Vice Provost for Graduate Education and Dean of the Graduate School
The University of Georgia
August 2025

DEDICATION

To my Lord and Savior Jesus Christ, this dissertation would not have been written if it were not for God giving me the wisdom and strength. I am nothing without God. To my family, I am forever indebted to you for your support through my educational journey. To my village of friends in every city I have ever lived or visited thank you for your support and love. Your motivation has encouraged me in more ways than you will ever know. And to my boyfriend Brandon, although we met at the end of my PhD, you have supported continuously, and I cannot wait to be able to support you in the way that you showed up for me. Thank you everyone. I love you for life.

ACKNOWLEDGEMENTS

To my adviser, Dr. Ron Orlando, thank you for allowing me to be a part of your research group and working through all of the challenges with me. You have taught me to think link a chef and critically analyze each step of the work. Some of my favorite memories during my time as a graduate student have been the impromptu conversations about any and everything, and I am grateful that you shared your knowledge with me. You have helped me grow into a scientist that is excited at the possibility of solving analytical challenges, and I cannot thank you enough for the way you have guided me. To Barry Boyes, thank you for sharing your knowledge of chromatography with me and giving me guidance on different projects and troubleshooting LC issues. To my committee members Dr. Jon Amster and Dr. Jeffery Urbauer who have believed me in every step of the way thank you.

Thank you to the University of Georgia Chemistry Department for giving me an opportunity. To the Complex Carbohydrate Research Center for all of the professors, lab managers, staff, and graduate students in the building who have supported me. Thank you for your support and wisdom. Thank you to all the former and current group members that have stayed late with me, helped me in their spare time, and have become my friends.

TABLE OF CONTENTS

Page

ACKNOWLEDGEMENTS v

CHAPTER

1 INTRODUCTION AND LITERATURE REVIEW 1

2 SEPARATING MONOSACCHARIDE STREOISOMERS VIA REDUCTIVE AMINATION AND ION MOBILITY MASS SPECTROMETRY (IM-MS) 19

3 ENANTIOMER SEPARATION OF D- AND L- AMINO ACIDS BY ION MOBILITY-MASS SPECTROMETRY (IM-MS) 43

5 ADVANCING HILIC RETENTION MODELING: CAN A RETENTION MODEL FOR N-GLYCANS BE DEVELOPED THAT APPLIES TO MULTIPLE STATIONARY PHASES? 67

6 EVALUATING THE MASS TRANSFER MECHANISM OF HILIC SPEARATIONS 89

7 CONCLUSICIONS 104

CHAPTER 1

INTRODUCTION AND LITERATURE REVIEW

Mass Spectrometry

Mass spectrometry is an analytical technique that ionizes compounds and analyzes their mass to determine their molecular weight, formula, and structure. It is a gas phase-based separation that can separate an analyte based on its mass to charge ratio and represented as m/z. The output of the signal from a mass spectrometer is displayed on a mass spectrum shown as a plot of ion abundance versus m/z which is representative of the mass in Daltons of the analyte. The mass is detected by a mass analyzer. A mass spectrometer consists of three main components the ion source, mass analyzer, and the detector[1]. Mass spectrometers can detect information of an analyte using minimal sample amount. Mass spectrometry has diverse applications across multiple disciplines, enabling the analysis of both pure substances and complex mixtures.

Ion Source

To get an analyte into the mass spectrometer they need to be ionized to enter into this gas-phase based separation/detection technique. An ion source is important to introduce energy into a molecule which allows ionization or to extract ionized materials from a solution. Traditional methods for ionization are called electron ionization (EI). Prior to EI, the analyte must be volatilized prior to entering the source. Followed by where a beam of energetic electrons ionize the analyte into either positive or negative electrons[2]. An electric field is then applied to the ions to pull the charged ions out of the

ion source. These ions can be either cations or anions. After ions are pulled out of the ion source, ions are guided into the mass analyzer where they are measured based on their mass to charge ratio (m/z) by a detector. EI is very useful as it is considered a "hard ionization" techniques[3] because it provides many fragment ions which can be helpful in identifying unknown compounds. A different type of electron ionization is a 'soft ionization" technique known as chemical ionization (CI). In CI, a chemical reaction occurs by using a reagent gas such as methane, or ammonia. As an example, ions are created by the collision of the sample vapor with ions of the reagent gas in the ion source[4].

The reagent gas is always present in large excess compared to the analyte to allow for selective ionization. The detection of these ions are usually intact mass due to mild ionization process. However, for unknown analytes the soft ionization could present as challenging to identify the sample due to the limited information that is received from the CI technique. Both of these techniques EI and CI are useful tools for chemist to perform analytical analysis and are most frequently coupled with gas chromatography.

For liquid chromatography, the most common ion source is electrospray ionization (ESI). This spray ionization technique occurs when an analyte is dissolved in a liquid and flowed through a tiny metal needle (nozzle)[5]. The tip of the nozzle has a strong electric charge that causes the liquid to break into tiny, charged droplets. Those droplets result in a fine mist which contains charged ions and uncharged ions and are released into the air or a vacuum[5]. The ions are pulled into the mass spectrometer and detected based on their m/z. This technique is very useful for highly polar analytes.

Mass Analyzers

There are many different mass analyzer types. Determining which mass analyzers are employed depends on the sample type and experiment performed. (Meaning what type of information one needs to gather). The most common types of analyzers in commercial production include quadrupole, ion trap, time-of-flight (TOF), and Fourier transform analyzers (ion cyclotron [ICR] and Orbitrap), along with numerous combinations or hybrids of these analyzers. The selection of a mass analyzer depends on factors such as resolution, scan speed, sensitivity, mass range, sample type, analysis speed, cost, and ionization method compatibility. Since no single analyzer excels in all aspects, the choice should be application specific. I will go over the background of each mass analyzer types principals and common application first starting with quadrupole.

A popular mass analyzer that is often used is a quadrupole due to its simplicity and ease of usage. Depending on the type of experiment a mass spectrometry may want to perform or depending on the sample type a quadrupole may be used. In practical terms the quadrupole consists of a set of four parallel electrodes (with a circular cross section) or hyperbolic rods parallel with each other [6]. It was designed by Dr. Paul Wolfgang in the 1950s to get the ions to separate the use of a direct current (DC) potential (U) is applied to two of the rods while the other two rods have an alternating frequency (rf) potential is applied[7]. This allows the ions that are ionized at the source to move in a pulse motion using an applied voltage. Ions which have a specific potential, frequency and are within a specified range of m/z will move towards the detector while the remaining ions will collide with the rods and fallout of trajectory.

This is all based on the Mathieu equation[8] . In addition to the use of most simple case of a quadrupole, the design can be improved by using additional pole rods like a hexapole or octupole which can be run in one mode of operation only such as RF-only and allow all ions to pass through. This design allows ions to move to an additional mass analyzer and act as a transmission guide. One can also induce collisions in the quadrupole under an inert gas which generate fragmented ions through collision induced dissociation (CID). Even though the quadrupole is a popular mass analyzer there is a disadvantage of its use. The mass range (usually <4000Da), low resolving power, and lack of its ability to perform MS/MS experiments limits its use. These disadvantages could be overcome by attaching a quadrupole to other analyzers such as additional quadrupoles (triple quadrupole instrument) or a quadrupole linked to a ToF (Q-Tof)[3].

Tandem Mass Spectrometry

Tandem mass spectrometry is a powerful technique that can be used to identify the sequence of peptides based on the fragment sequence selected from precursor ions[9]. Fragment ions show characteristics of the chemical structure of the precursor ion[10]. The process of tandem mass spectrometry consist of ionizing a sample by an ionization source, soft ionization techniques are employed most commonly electrospray ionization and then ions are analyzed by the first mass analyzer. In the first mass analyzer a precursor ion is selected, the selected ion is then sent to the collision cell and fragmented by a neutral gas (usually Argon)[11]. While in the collision cell the ions are excited by collision with the target gas by a process known as collision induced dissociation[26]. Fragment ions are generated and then sent to the second mass analyzer and a mass

spectrum is generated. A modification of the quadrupole mass analyzer is the ion trap. This mass analyzer is the most commonly used ion trap instrument.

Detector

In a mass spectrometer, the detector is the final component that measures and counts ions by detecting the electrical signals they produce [12]. It only detects charged particles[13]. Any neutral molecules that don't carry a charge are not detected and are instead removed by the vacuum inside the system[14]. One of the most common detectors is the electron multiplier. It is widely used due to its ability to amplify signal and accelerate to measure m/z. The electron multiplier (EM) operates in a vacuum-sealed environment, allowing charged analyte ions to strike its internal surface[15]. This impact releases a small number of electrons, known as primary emission[16]. These electrons then strike other surfaces within the tube, generating additional secondary electrons in a cascading effect[17]. This multiplication process produces an amplified electrical signal that can be detected and used to identify the ion. The strength of the signal is dependent on the number of ions that initially enter the EM[18]. There are two main types of electron multipliers, the discrete-dynode and the continuous-dynode[19]. The discrete-dynode EM operates when a charged ion strikes the first dynode, and a few electrons are knocked out[20].

Those electrons are then accelerated to the next dynode and hit and knock out more electrons[21]. The process repeats through multiple dynodes and allow for the signal to be amplified at each stage for gains of about 10^8 electrons[16]. For continuous dynodes, there is only one curved tube with a glass coating of semiconducting material[22]. The ions strike the inner wall of the tube and cause electrons to be released. Those electrons spiral

down the tube and the hit the wall causing collisions and more electrons are released creating a cascade of signals. This allows for a gain of 10^6 electrons[23]. Continuous-dynode electron multipliers can also be designed in a different geometry known as a microchannel plate (MCP)[24]. An MCP is essentially a two-dimensional array of thousands of tiny continuous-dynode electron multipliers arranged in parallel [25]. Each microchannel is a narrow, hollow tube made from lead glass and coated with a semiconductive layer on the inside[26]. When an ion or electron enters a channel, it triggers a cascade of secondary electrons, resulting in a signal gain of approximately 10^4 to 10^7 electrons per channel[24].

Ion Mobility

Ion mobility (IM) is an analytical technique that separates gas-phase ions based on their shape, size, and charge as they drift through an inert gas[25]. The degree of interaction between each ion and the gas molecules affects how quickly the ion travels. This separation is quantified as a collision cross section (CCS). It is widely used in security and defense to detect substances like explosives and drugs[26], IMS also has broad applications in laboratory research, including the analysis of both small and large biomolecules[27]. Although IMS can function independently with high sensitivity, it is frequently combined with methods such as mass spectrometry, gas chromatography, or liquid chromatography to enhance separation capabilities. The size and design of IMS devices vary depending on their purpose, from compact, handheld systems to large-scale instruments.

Liquid Chromatography

Liquid chromatography (LC) is an analytical technique developed in the early 1900s that separates components in a mixture based on their differential interactions with a stationary phase and a liquid mobile phase[28]. As the mobile phase flows through a packed column, analytes distribute between the stationary and mobile phases depending on their physicochemical properties[29]. These interactions affect the speed at which each analyte travels through the column, resulting in their separation over time[30]. The greater an analyte's affinity for the stationary phase, the slower it moves; conversely, analytes that interact more with the mobile phase elute faster. Because of these selective interactions, LC enables the resolution of complex mixtures into individual components. Over the past century, the technique has advanced significantly. Today, LC includes specialized forms such as capillary LC, microbore LC, high-performance liquid chromatography (HPLC), and preparative LC, each tailored for different analytical or preparative needs.

Principles of Liquid Chromatography

Chromatographic separation is driven by how different compounds interact with the stationary phase[32]. The difference in retention behavior ultimately determines how well two analytes can be resolved. These interactions are rooted in thermodynamic principles, reflecting the affinity of each compound for the stationary versus mobile phases[33]. In contrast, column efficiency describes how sharply each analyte band travels through the column, which is influenced by kinetic factors such as diffusion and mass transfer[34]. Selectivity, often expressed as the separation factor (α), provides a measure of how distinctly two compounds are retained[35]. Efficiency, on the other hand, is typically

reported as the number of theoretical plates (N) or plate height (H)[36]. To achieve good separation, both selectivity and efficiency must be optimized, this involves not only choosing the right stationary phase but also fine-tuning system parameters like flow rate, temperature, and column dimensions. The concept of theoretical plates is commonly used to describe column efficiency in chromatography. It serves as a way to quantify how well a column can separate different analytes. Higher plate numbers generally indicate sharper peaks and better resolution. The number of theoretical plates, denoted as N, can be calculated using the analyte's retention time and the width of the peak at half its height, following the equation[37]:

$$N = 5.545 * \left(\frac{t_r}{w_h}\right)^2$$

where t_r refers to the retention time of the peak and w_h refers to the peak width at half height. A higher N value reflects more efficient separation. This framework is useful when evaluating column performance and making method adjustments to improve resolution.

Advancements in LC- HPLC

High performance liquid chromatography (HPLC) is most commonly used in proteomic workflows to help with resolution and identification of as many peptide sequences by the mass spectrometer. Separation in HPLC is based on the peptide's interaction with the stationary phase (column) and the mobile phase (solvent gradient elution). The most extensively used technique to separate peptides in bottom-up proteomics uses strong cation-exchange (SCX) chromatography and then reversed-phase (RP) LC-MS/MS[31]. The principle of this is by separating peptides based on their charge

and then hydrophobicity. SCX chromatography can be directly coupled with RP chromatography or off-line[31].

Reversed-Phase Chromatography

A separation mode which can separate analytes based on their hydrophobicity. The stationary phased used in reverse phase liquid chromatography (RPLC) is a when you have a non-polar stationary phase and usually a non-polar stationary phase. Most separations of biological analysis are performed by RP as the sample components are separated based on the hydrophobicity. The stationary phase in reversed-phase liquid chromatography is typically made of silica particles that are chemically modified with hydrophobic alkyl chains such as C18 or C8. These modifications make the stationary phase non-polar. The choice of stationary phase is critical because it directly influences how effectively analytes are separated. One key factor is the length of the alkyl chains attached to the silica surface—longer chains (e.g., C18) result in a more hydrophobic stationary phase, which increases retention of non-polar analytes. In contrast, shorter chains (e.g., C8) make the phase less hydrophobic, allowing for faster elution of certain compounds. Therefore, selecting the appropriate stationary phase based on hydrophobicity is essential for optimizing separation based on the analyte's properties.

Hydrophilic Interaction Liquid Chromatography (HILIC)

Hydrophilic interaction liquid chromatography (HILIC) is a form of normal-phase chromatography[38] that has gained widespread use, especially for separating polar compounds. While it shares some conceptual overlap with reversed-phase and ion chromatography, HILIC distinguishes itself by employing a hydrophilic stationary phase in combination with eluents that resemble those used in reversed-phase systems typically

high in organic solvent with a small amount of aqueous buffer. Originally introduced by Andrew Alpert in 1990[40], HILIC was described as a liquid-liquid partitioning mechanism where analytes elute in order of increasing polarity[41]. Since then, this understanding has been supported and refined through continued experimental work[42].

Although a variety of polar stationary phases can be used, HILIC materials are commonly grouped into five main types[43]: unbonded silica or diol-based phases, amino or anion-exchange phases, amide-functionalized surfaces, cationic materials, and zwitterionic phases. In some cases, even reversed-phase materials with exposed silica sites can support HILIC-like interactions under high organic solvent conditions. HILIC has proven especially valuable for metabolomics and glycomics applications due to its strong retention of polar metabolites and carbohydrates, as well as its compatibility with electrospray ionization mass spectrometry[44]. The high organic solvent content often leads to enhanced MS sensitivity sometimes by an order of magnitude compared to reversed-phase methods. This makes it particularly well-suited for analyzing polar biomolecules such as glycoproteins, glycans, and metabolites in complex biological samples[45].

Zwitterionic Chromatography

Zwitterionic stationary phases have become an important class of materials in HILIC, gaining popularity early on due to their balanced selectivity and unique surface chemistry[46]. These phases are designed to carry both positive and negative charges within the same functional group, ideally resulting in an overall neutral surface. Despite this neutrality, the close proximity of the opposing charges allows for subtle electrostatic interactions that can influence selectivity without dominating the retention mechanism[47]. One of the most common zwitterionic groups used is the sulfobetaine moiety, which

features a quaternary ammonium and a sulfonic acid. Because both are strong ion-exchange groups, this functionality maintains a "charged but neutral" character regardless of the mobile phase pH[48]. Recent developments in zwitterionic materials have focused on modifying retention strength and hydrophilicity. For instance, a study exploring a trimethylchlorosilane-capped zwitterionic phase incorporating a 3-P,P-diphenylphosphoniumpropylsulfonate group showed reduced retention at pH 4.1 under low buffer conditions[49].

The capping appeared to reduce the influence of exposed silanols, which otherwise contribute to hydrophilicity and possibly unintended retention due to steric effects. These results suggest that the introduction of hydrophobic or sterically bulky end groups can disrupt the water-rich partitioning layer that underpins the HILIC mechanism, leading to weaker retention[49]. Other zwitterionic systems have also emerged, including phases based on lysine-functionalized silica monoliths, which offered stronger HILIC retention than traditional diol monoliths[50]. Polymeric zwitterionic monoliths have also been explored, and more recently, commercial options such as Merck's CapRod ZIC-HILIC have brought sulfobetaine -functionalized monolith capillaries into broader use[51]. It's important to note that the apparent "charge" behavior of a column is influenced not only by the bonded functional group, but also by factors like pH and the base silica material. Even so-called neutral phases may exhibit weak ion-exchange behavior due to residual silanol groups. Likewise, zwitterionic groups, especially weak ones which can be sensitive to mobile phase conditions, which may shift their interaction profiles depending on buffer strength and pH.

References

1. Sorribes-Soriano, de, M., Esteve-Turrillas, F. A., & Armenta, S. (2018). Trace analysis by ion mobility spectrometry: From conventional to smart sample preconcentration methods. A review. Analytica Chimica Acta, 1026, 37–50.
2. Ahn, J., Bones, J., Ying Qing Yu, Rudd, P. M., & Gilar, M. (2010). Separation of 2-aminobenzamide labeled glycans using hydrophilic interaction chromatography columns packed with 1.7μm sorbent. Journal of Chromatography B, 878(3-4), 403–408.
3. Allen, J. S. (1947). An Improved Electron Multiplier Particle Counter. Review of Scientific Instruments, 18(10), 739–749.
4. Alpert, A. J. (1990). Hydrophilic-interaction chromatography for the separation of peptides, nucleic acids, and other polar compounds. Journal of Chromatography A, 499, 177–196.
5. Baković, M. P., Selman, M. H. J., Hoffmann, M., Rudan, I., Campbell, H., Deelder, A. M., Lauc, G., & Wuhrer, M. (2013). High-Throughput IgG Fc N-Glycosylation Profiling by Mass Spectrometry of Glycopeptides. Journal of Proteome Research, 12(2), 821–831.
6. Bij, K. E., Horváth, C., Melander, W. R., & Nahum, A. (1981). Surface silanols in silica-bonded hydrocarbonaceous stationary phases. Journal of Chromatography A, 203, 65–84.

7. Boggess, B. (2001). Mass Spectrometry Desk Reference (Sparkman, O. David). Journal of Chemical Education, 78(2), p.168.
8. Burroughs, E. G. (1969). Collection Efficiency of Continuous Dynode Electron Multiple Arrays. Review of Scientific Instruments, 40(1), 35–37.
9. Buszewski, B., & Noga, S. (2011). Hydrophilic interaction liquid chromatography (HILIC)—a powerful separation technique. Analytical and Bioanalytical Chemistry, 402(1), 231–247.
10. Carlson, R. W. (2025). Thermal ionization mass spectrometry. Treatise on Geochemistry, 8, 473–496.
11. Coskun, O. (2016). Separation techniques: Chromatography. Northern Clinics of Istanbul, 3(2), 156–160. National Library of Medicine.
12. Amunugama, R., Jones, R., Ford, M. and Allen, D., 2013. Bottom-Up Mass Spectrometry–Based Proteomics as an Investigative Analytical Tool for Discovery and Quantification of Proteins in Biological Samples. Advances in Wound Care, 2(9), pp.549-557.
13. Doran, P. M. (1995). Unit Operations. Bioprocess Engineering Principles, 218–253.
14. El-Aneed, A., Cohen, A., & Banoub, J. (2009). Mass Spectrometry, Review of the Basics: Electrospray, MALDI, and Commonly Used Mass Analyzers. Applied Spectroscopy Reviews, 44(3), 210–230.
15. Elliott, A. G., Merenbloom, S. I., Chakrabarty, S., & Williams, E. R. (2017). Single Particle Analyzer of Mass: A Charge Detection Mass Spectrometer with a

Multi-Detector Electrostatic Ion Trap. International Journal of Mass Spectrometry, 414, 45–55.

16. Ettre, L. S. (1993). Nomenclature for chromatography (IUPAC Recommendations 1993). Pure and Applied Chemistry, 65(4), 819–872.
17. Garg, E., & Zubair, M. (2024). Mass Spectrometer. In StatPearls. StatPearls Publishing.
18. Gillet, L.C., Leitner, A. and Aebersold, R. (2016). Mass Spectrometry Applied to Bottom-Up Proteomics: Entering the High-Throughput Era for Hypothesis Testing. Annual Review of Analytical Chemistry, 9(1), pp.449–472.
19. Glish, G. L., & Vachet, R. W. (2003). The basics of mass spectrometry in the twenty-first century. Nature Reviews Drug Discovery, 2(2), 140–150.
20. Griffiths, J. (2008). A Brief History of Mass Spectrometry. Analytical Chemistry, 80(15), 5678–5683.
21. Guo, Y., & Gaiki, S. (2011). Retention and selectivity of stationary phases for hydrophilic interaction chromatography. Journal of Chromatography A, 1218(35), 5920–5938.
22. Gys, T. (2015). Micro-channel plates and vacuum detectors. Nuclear Instruments and Methods in Physics Research Section A: Accelerators, Spectrometers, Detectors and Associated Equipment, 787, 254–260.
23. Hage, D. S. (2018). Chromatography. Principles and Applications of Clinical Mass Spectrometry, 1–32.
24. Hemström, P., & Irgum, K. (2006). Hydrophilic interaction chromatography. Journal of Separation Science, 29(12), 1784–1821.

25. Huang, G., Lian, Q., Zeng, W., & Xie, Z. (2008). Preparation and evaluation of a lysine-bonded silica monolith as polar stationary phase for hydrophilic interaction pressurized capillary electrochromatography. ELECTROPHORESIS, 29(18), 3896–3904.
26. Jandera, P. (2011). Stationary and mobile phases in hydrophilic interaction chromatography: a review. Analytica Chimica Acta, 692(1-2), 1–25.
27. Jiang, Z., Smith, N. W., & Liu, Z. (2011). Preparation and application of hydrophilic monolithic columns. Journal of Chromatography A, 1218(17), 2350–2361.
28. Jr, M. J. (2000). Organic Chemistry. W. W. Norton.
29. Kaake, R. M., Wang, X., Burke, A. J., Yu, C., Wynne Kandur, Yang, Y.-Y., Novtisky, E. J., Tonya Pekar Second, Duan, J., Kao, A., Guan, S., Vellucci, D., Rychnovsky, S. D., & Huang, L. (2014). A New in Vivo Cross-linking Mass Spectrometry Platform to Define Protein–Protein Interactions in Living Cells. 13(12), 3533–3543.
30. Koh, D., Park, J., Lim, J., Yea, M.-J., & Bang, D. (2018). A rapid method for simultaneous quantification of 13 sugars and sugar alcohols in food products by UPLC-ELSD. Food Chemistry, 240, 694–700.
31. Ladislas Wiza, J. (1979). Microchannel plate detectors. Nuclear Instruments and Methods, 162(1-3), 587–601.
32. Liu, B., Li, J., Chen, S., Yang, J., Hu, W., Tian, J., & Wu, S. (2024). Performance improvement of a discrete dynode electron multiplication system through the optimization of secondary electron emitter and the adoption of double-grid

dynode structure. Nuclear Instruments and Methods in Physics Research Section a Accelerators Spectrometers Detectors and Associated Equipment, 1062(1062), 169162–169162.

33. MäkinenM. A., Anttalainen, O. A., & SillanpääM. E. T. (2010). Ion Mobility Spectrometry and Its Applications in Detection of Chemical Warfare Agents. Analytical Chemistry, 82(23), 9594–9600.
34. March, R. E., & Hughes, R. J. (1989). Quadrupole Storage Mass Spectrometry. Wiley-Interscience.
35. Märk, T. D., & Dunn, G. H. (2013). Electron impact ionization. Springer.
36. Miller, P. E., & Denton, M. B. (1986). The quadrupole mass filter: Basic operating concepts. Journal of Chemical Education, 63(7), 617.
37. Munson, B., & Field, F. H. (1966). Chemical Ionization Mass Spectrometry. I. General Introduction. Journal of the American Chemical Society, 88(12), 2621–2630.
38. Nakorchevsky, A., & Yates, J. R. (2012). 1.17 Mass Spectrometry. Www.sciencedirect.com, 1(2012), 341–375.
39. Naylor, C. N., & Nagy, G. (2024). Recent advances in high-resolution traveling wave-based ion mobility separations coupled to mass spectrometry. Mass Spectrometry Reviews, 44(4).
40. Pagnotti, V. S., Chubatyi, N. D., & McEwen, C. N. (2011). Solvent Assisted Inlet Ionization: An Ultrasensitive New Liquid Introduction Ionization Method for Mass Spectrometry. Analytical Chemistry, 83(11), 3981–3985.

41. Palamareva, M. D. (2005). LIQUID CHROMATOGRAPHY | Principles. Encyclopedia of Analytical Science, 112–118.
42. Popecki, M. A., Adams, B., Craven, C. A., Cremer, T., Foley, M. R., Lyashenko, A., O'Mahony, A., Minot, M. J., Aviles, M., Bond, J. L., Stochaj, M. E., Worstell, W., Elam, J. W., Mane, A. U., Siegmund, O. H. W., Ertley, C., Kistler, L. M., & Granoff, M. S. (2016). Microchannel plate fabrication using glass capillary arrays with Atomic Layer Deposition films for resistance and gain. Journal of Geophysical Research: Space Physics, 121(8), 7449–7460.
43. Qiao, L., Dou, A., Shi, X., Li, H., Shan, Y., Lu, X., & Xu, G. (2013). Development and evaluation of new imidazolium-based zwitterionic stationary phases for hydrophilic interaction chromatography. Journal of Chromatography A, 1286, 137–145.
44. Qiu, H., Wanigasekara, E., Zhang, Y., Tran, T., & Armstrong, D. W. (2011). Development and evaluation of new zwitterionic Hydrophilic interaction liquid chromatography stationary phases based on 3-P,P-diphenylphosphonium-propylsulfonate. Journal of Chromatography A, 1218(44), 8075–8082.
45. Schweiger, S., Hinterberger, S., & Jungbauer, A. (2017). Column-to-column packing variation of disposable pre-packed columns for protein chromatography. Journal of Chromatography A, 1527, 70–79.
46. Skoog, D. A., F James Holler, & Crouch, S. R. (2007). Principles of instrumental analysis. Thomson Brooks/Cole.
47. Stauffer, E., Dolan, J. A., & Newman, R. (2008). Gas Chromatography and Gas Chromatography—Mass Spectrometry. Fire Debris Analysis, 235–293.

48. TALAS, E., & DUMAN, M. (2023). Comparison of Grain Size Trend Analysis and Multi-Index Pollution Assessment of Marine Sediments of the Gülbahçe Bay, Aegean Sea. International Journal of Environment and Geoinformatics, 10(2), 159–179.
49. Tanner, M. A., & Detlef Günther. (2009). Short transient signals, a challenge for inductively coupled plasma mass spectrometry, a review. Analytica Chimica Acta, 633(1), 19–28.
50. Tao, S. X., Chan, H. W., & van der Graaf, H. (2016). Secondary Electron Emission Materials for Transmission Dynodes in Novel Photomultipliers: A Review. Materials, 9(12), 1017.
51. Wohlgemuth, J., Karas, M., Jiang, W., Hendriks, R., & Sven Andrecht. (2010). Enhanced glyco-profiling by specific glycopeptide enrichment and complementary monolithic nano-LC (ZIC-HILIC/RP18e)/ESI-MS analysis. Journal of Separation Science, 33(6-7), 880–890.

CHAPTER 2

SEPARATING MONOSACCHARIDE STEREOISOMERS VIA REDUCTIVE AMINATION AND ION MOBILITY MASS SPECTROMETRY (IM-MS)

1 Brown, M., Orlando, R. To be submitted to a peer-reviewed journal

Abstract

Monosaccharides exist in multiple stereochemical configurations. Their absolute configuration plays a role in biological function and molecular recognition. For example, aldohexoses contain four chiral centers, giving rise to 16 possible stereoisomers—eight D-isomers and eight L-isomers—with D-hexoses predominating in nature. Stereoisomers are challenging to separate due to their structural similarities; they can present as an analytical challenge. A technique to overcome this challenge is to derivatize the monosaccharides with a chiral tag enabling separation coupled with using ion mobility mass spectrometry (IM-MS). Derivatizing with a chiral molecule enable separation and ion mobility provides a high throughput approach for separating these stereoisomers. This method can be used as a tool for glycosylation characterization.

Keywords: High resolution ion mobility–mass spectrometry, Monosaccharides, Stereoisomers, Reductive amination, Chiral separation

Introduction

Monosaccharides are essential building blocks of complex carbohydrates, glycoconjugates, and polysaccharides[2]. Their structural diversity is critical for various biological processes, including cell-cell recognition, immune response modulation, and metabolic regulation[3,4,19]. Despite their relatively simple chemical compositions, monosaccharides are complex structures which have multiple stereocenters. This complexity results in numerous isomeric forms, including constitutional isomers, epimers, and anomers. The multiple isomeric forms can impact biological function, reactivity, and recognition by enzymes and receptors[3]. Characterization of these isomers are necessary in fields such as glycomics, food science, and pharmaceutical research[5,6,20].

Separation of monosaccharide stereoisomer is necessary for enantiomer and diastereomer discrimination. Enantiomers are pairs of stereoisomers that are non-superimposable mirror images of each other and share identical physical properties, such as solubility, boiling point and melting point. As a result they cannot be resolved by common physical techniques such as crystallization, distillation or conventional chromatography[2]. A widely used approach involves gas chromatography–mass spectrometry (GC-MS), which is considered the golden standard7 for chiral analysis. This method converts enantiomers into diastereomers through acid-catalyzed derivatization with optically pure reagents, such as 2-octanol or 2-butanol[3]. The resulting derivatives must then be converted to become volatile.

Gas chromatography (GC) can use multiple derivatization strategies, to enhance the volatility and detectability of monosaccharides, with silylation and acetylation being among the most widely used methods. Trimethylsilyl (TMS) derivatization was first recommended for sugar analysis by Knapp et al. in 1979, although this approach often produces multiple isomeric forms, resulting in complex chromatographic patterns[6]. More recent studies, such as that by Haas et al. (2018), have incorporated an oximation step prior to TMS or trifluoroacetyl (TFA) derivatization, which limits the formation to two isomers and improves chromatographic resolution[11]. However, oximation followed by TFA or TMS derivatization, while broadly applicable and straightforward, may still pose challenges for accurate quantification due to the presence of multiple isomers. In contrast, alditol acetylation reduces the carbonyl group to a hydroxyl, eliminating cyclization and thereby simplifying the isomeric profile, but this transformation can obscure original enantiomeric information [6,7]. Several GC-based methods have been developed to minimize isomer formation, including oxime generation [8,10,14] and reduction of aldoses to their corresponding alditols[15]. These derivatization strategies play a critical role in the separation of monosaccharide diastereomers but yet diastereomeric separation remains particularly challenging and often requires additional optimization.

Monosaccharide diastereomers, a class of stereoisomers with non-superimposable and non-mirror image configurations, possess distinct physical properties that allow for chromatographic separation. Gas chromatography–mass spectrometry (GC-MS) is frequently employed for this purpose under optimized derivatization conditions. The choice of derivatization strategy plays a critical role in enhancing diastereomer resolution, as it directly influences molecular volatility, polarity, and steric interactions.

However, even with appropriate derivatization, structurally similar diastereomers can exhibit overlapping retention times, resulting in poorly resolved chromatographic peaks. These limitations are particularly evident when analyzing mixtures containing sugars with minimal stereochemical differences. Although GC-MS provides robust analytical capabilities, it still faces challenges in sensitivity, resolution, and sample preparation complexity, especially for high-throughput or structurally diverse carbohydrate analyses.

Chiral derivatization combined with ion mobility–mass spectrometry (IM-MS) provides an alternative strategy for resolving monosaccharide stereoisomers. IM-MS separates ions based on their size, shape, charge, and mass in the gas phase, offering an additional dimension of separation which can help in resolving structurally similar molecules[13]. Reductive amination with optically pure reagents enables chiral tagging at the C-1 aldehyde position of aldohexoses, breaking the symmetry in the monosaccharide and allowing separation of enantiomers [14,22]. The chiral derivation group should be carefully considered as the selection of the group can affect ion mobility separation.

The objective of this study is to explore the application of IM-MS for the separation of monosaccharide isomers derivatized with an amino acid. This approach using chiral derivatization and IM-MS to separate isomeric species that are traditionally difficult to separate using conventional chromatographic techniques, including the simultaneous separation of D- and L-enantiomers as well as aldohexose diastereomers in one experiment.

Materials and Methods

Instrumentation and Separation conditions

Experiments were performed using a high resolution ion mobility (HRIM) MOBIE device (MOBILion Systems, Chadds Ford, PA, USA). The HRIM device was coupled to an Agilent 6546 quadrupole time-of-flight (QTOF) mass spectrometer (Agilent Technologies, Santa Clara, CA, USA). Samples were ionized using the Agilent Dual Jet Stream Source (Dual AJS) ion source with positive polarity. Agilent MassHunter software (ver. B.11.0) was used for MS system control. MOBILion's EyeOn software (ver. 1.5) was used to control the SLIM system and for IM-MS data acquisition.

Sample introduction was performed using an Agilent 1290 Infinity II LC stack (Agilent Technologies, Santa Clara, CA, USA) using a 2.1 x 150 mm Halo penta-HILIC column packed with 2.7-µm diameter superficially porous particles (Advanced Materials Technology, Wilmington, DE, USA). The column and sample temperatures were maintained at 10 °C and 60 °C, respectively. The eluent consisted of 50mM ammonium formate with 0.1% formic acid (A) and acetonitrile with 0.1% formic acid (B). Analysis was performed using the following gradient elution 80 to 40B over 10 min at a flow rate of 0.20 mL/min. The analysis was followed by a 5-min washing procedure with 10% A and a re-equilibration period of 5 min. All solutions were filtered through 0.20-µm membrane filters, and the injection volume was 10 µL. The total run time for analysis was 20-min.

The SLIM chamber was maintained at 2.5 Torr for all experiments. Ions were trapped in an accumulation region on the SLIM board, followed by release and separation in the separation region of the board[15], which consists of a 13 m serpentine pathway. The traveling wave frequency and amplitude used for the experiments were 15 kHz and 30 Vp-p, respectively.

The LC-HRIM-MS data are recorded in mbi data format and converted to the Agilent IM-MS MassHunter data format (.d) using MOBILion's HRIM Data Processor software (ver. 1.10.29.1). The PNNL preprocessor software (ver. 4.0) was used for drift bin compression (2:1) and drift dimension smoothing for enhanced signal quality

Chemicals and samples

Monosaccharide standards including D-glucose, D-galactose, D-N-acetylgalactosamine, D-N-acetylglucosamine, D-fucose, L-fucose, D-talose, D-allose, D-altrose, and D-gulose were purchased from Sigma Aldrich (St. Louis, MO, USA). L-glucose, L-galactose, and D-mannose were purchased from Thermo Fisher Scientific (Waltham, MA, USA); L-altrose and D-gulose from Toronto Research Chemicals Inc. (Vaughan, ON, Canada); and L-talose, L-allose, L-altrose, and L-gulose from Ambeed Inc. (Buffalo Grove, IL, USA). Purity of monosaccharide standards were in the range 95–99%. Acetonitrile, water, and formic acid are HPLC grade and purchased from Thermo Fisher Scientific, Waltham, MA, USA.

Reductive Amination Labeling Strategy/ Derivatization of Aldohexoses

All monosaccharides were tagged with Procainamide labeling with sodium cyanoborohydride (NaBH3CN) reductive amination. For derivatization, 200 µL of a labeling solution containing 0.4 M Procainamide HCl and 0.8 M sodium cyanoborohydride ($NaBH_3CN$) in dimethyl sulfoxide:acetic acid:water (7:2:1, v/v) was added to each monosaccharide sample. The mixture was incubated at 65°C overnight. After which samples were dried using a speed vacuum with no heat. The vacuum dried sample was resuspended in 5% acetic acid (240µL) and cleaned on a PD MiniTrap G10 desalting column (Cytiva, Marlborough, MA, USA) using the manufacturer's protocol.

The samples were then speed vacuumed and resuspended in 100% H20 (1 mg/mL) for LC-MS analysis.

Results/Discussion

This work evaluated the ability to differentiate monosaccharide stereoisomers using chiral derivatization and IM-MS. Chiral derivatization using an amino acid was performed using reductive amination. This step was vital to enable separation of monosaccharide stereoisomers. This section will discuss the analytical techniques used, the reductive amination chemistry, how the chiral tag was selected, followed by the monosaccharide stereoisomer separation.

Reductive Amination

Reductive amination was used to derivatize monosaccharides and enable stereoisomer separation by ion mobility–mass spectrometry (IM-MS). The reaction occurs at the aldehyde group on the C-1 carbon, where a chiral amine forms an imine (Schiff base) intermediate that is after reduced to a stable secondary amine. This modification introduces a new chiral center at the derivatization site, converting enantiomers into diastereomers with distinctive gas-phase structures.

This structural difference allows for separation in the ion mobility cell. The derivatization tag must contain a primary amine, limiting candidate molecules to compounds such as amino acids. Sodium cyanoborohydride ($NaBH_3CN$) was selected as the reducing agent because it is effective under mildly acidic conditions (~pH 3–4) and selectively reduces imines without interfering with unreacted aldehyde groups. Following derivatization, multiple amino acid tags were selected to determine their effectiveness in resolving stereoisomers by IM-MS. To identify the most effective amino acid for

separation, multiple amino acids where considered. Each amino acid was evaluated for its ability to maximize the ion mobility separation.

Selection of derivatization tag

Tag selection was an important step for enabling stereoisomer separation. The ideal tag needed to contain a primary amine for reductive amination, ionize efficiently under electrospray conditions, and introduce an additional chiral center to induce structural differences for enantiomeric separation. As demonstrated in GC-MS analysis of monosaccharides, the use of an optically pure derivatizing agent is necessary to determine the absolute configuration, as it introduces asymmetry and prevents the formation of racemic mixtures18. These criteria led to the consideration of amino acids as candidates.

Initial experiments focused on amino acids with basic side chains. Arginine was evaluated due to its guanidinium group which promotes ionization in positive-mode electrospray. IM-MS analysis showed multiple peaks in the mobiligram of D- and L-glucose stereoisomers (Figure 2.1). This was likely to due to the presence of multiple reactive sites. Multiple peaks for a single enantiomer created overlap with the second enantiomer, making it difficult to distinguish between the two and potentially leading to misidentification in unknown mixtures. Lysine was excluded from further testing because it also contains multiple reactive sites that could cause similar issues. Histidine was evaluated with glucose enantiomers. Despite having a single primary amine, histidine-tagged derivatives did not show any measurable separation (Figure 2.2). This result suggested that amino acids with small or compact side chains do not induce sufficient structural differences for separation in the ion mobility cell. Tyrosine was selected due to

its bulky aromatic side chain and single reactive amine. IM-MS analysis of tyrosine-derivatized glucose showed a 4.4 ms separation between D- and L-glucose (Figure 2.3). This result indicated that the side chain's steric bulk contributes to enhanced separation and supported the use of tyrosine for further evaluation of additional monosaccharide stereoisomers.

IM-MS Separation

Tyrosine-derivatized monosaccharides were evaluated to determine whether IM-MS could separate D- and L-aldohexose stereoisomers. Seven of the eight aldohexoses were evaluated, and each derivative formed a [M+H]+ ion at m/z 346.2. Derivatization with a chiral tag such as tyrosine enabled separation of all enantiomeric pairs (Table 2.1). Trends in separation were observed among epimeric pairs. Epimers that differed at the C-2 position, such as D-glucose and D-mannose (Figure 2.4) and D-galactose and D-talose (Figure 2.5), showed the most distinct separation. Epimers with stereocenter differences further from the derivatization site displayed lower resolution, indicating that ion mobility separation is influenced by the location of the chiral center relative to the tag.

Additional sugar classes were also examined using the same derivatization approach. D- and L-fucose, a deoxyhexose sugar, were successfully separated following tyrosine labeling (Figure 2.6). Structural isomers of N-acetylated sugars, including N-acetylglucosamine and N-acetylgalactosamine, were also resolved under the same conditions (Figure 2.7). These results demonstrated that the strategy was effective beyond aldohexoses and could potentially be extended to modified monosaccharides containing deoxy or N-acetyl functional groups. This finding prompted further evaluation of the method for compositional analysis using mixed monosaccharide samples.

Compositional analysis was performed to evaluate if tyrosine derivatization combined with IM-MS could resolve mixtures of monosaccharide isomers. A standard mixture containing D-mannose, talose, altrose, and glucose was prepared and derivatized. Each component produced a [M+H]+ ion at m/z 346.2, and separation was assessed based on arrival time differences in the ion mobility cell. Results from this experiment (Figure 2.8) showed separation of most standards, except in cases where the epimerization site was located further from the derivatization site. Lower resolution was observed when the stereocenter was positioned farther from the C-1 carbon, where the chiral tag was introduced, consistent with trends seen in individual epimer pairs. This limitation indicates that ion mobility separation becomes less effective for distinguishing structural isomers when conformational changes are further away from the tagged site. Although baseline separation was not achieved for every sugar in the mixture, the method still enabled separation of most components without the need for chromatographic separation.

Conclusion

This work demonstrated that D- and L-monosaccharides can be derivatized using amino acids, particularly those with aromatic side chains such as tyrosine, to enable separation by ion mobility–mass spectrometry (IM-MS). Reductive amination introduced a new stereocenter at the C-1 position, converting enantiomers into diastereomers that could be resolved in the gas phase. All seven aldohexoses evaluated were successfully separated following derivatization with tyrosine. Separation trends among epimers showed that resolution improved when the stereocenter was closer to the derivatization site. Lower resolution was observed for epimers that differed at positions further from C-

1, indicating a distance-dependent effect on gas-phase separation. In addition to aldohexoses, the method also resolved other sugar classes, including D- and L-fucose and N-acetylated isomers such as N-acetylglucosamine and N-acetylgalactosamine.

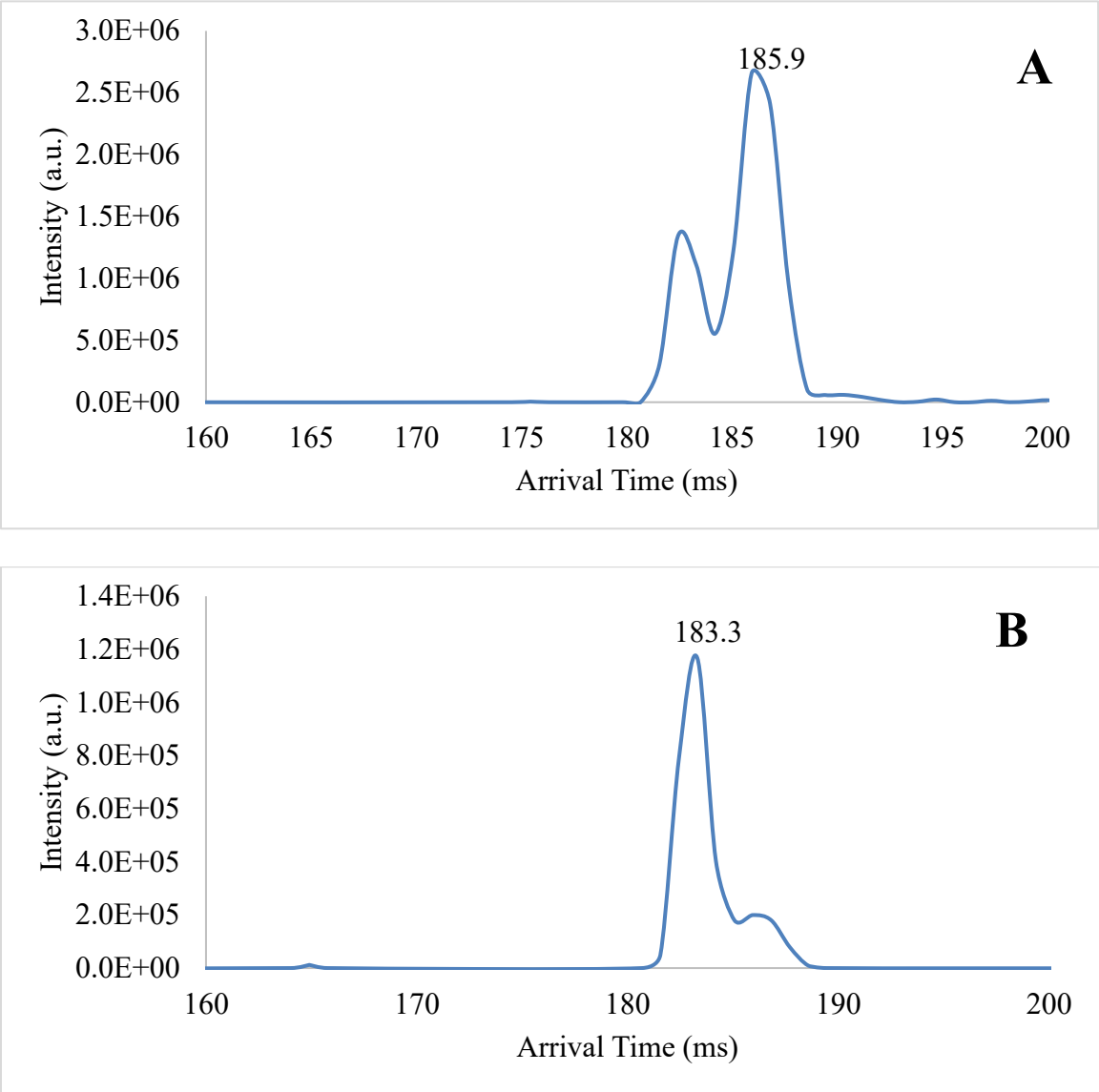

Figure 2.1 Displays the extracted mobiligrams for the protonated molecular ion ($[M+H]^+$ at 339.16 m/z) for L-and D- glucose derivatized with L-arginine. (A) displays results from the L-isomer and (B) the D-isomer.

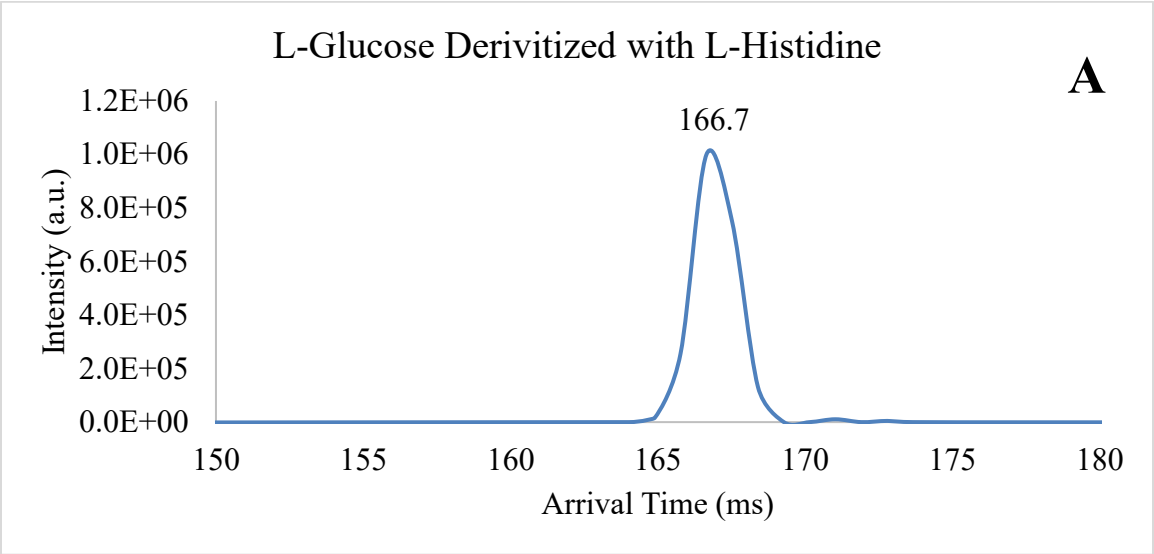

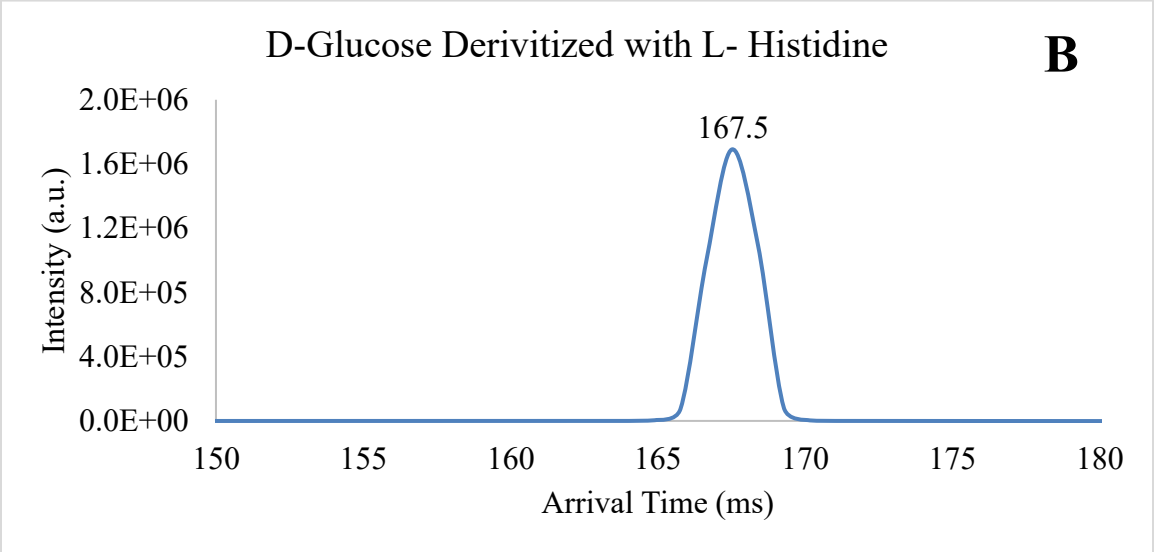

Figure 2.3 Extracted mobiligram for 320.12 $[M+H]^+$ for L- glucose (A) and D-glucose (B) derivatized with L-histidine.

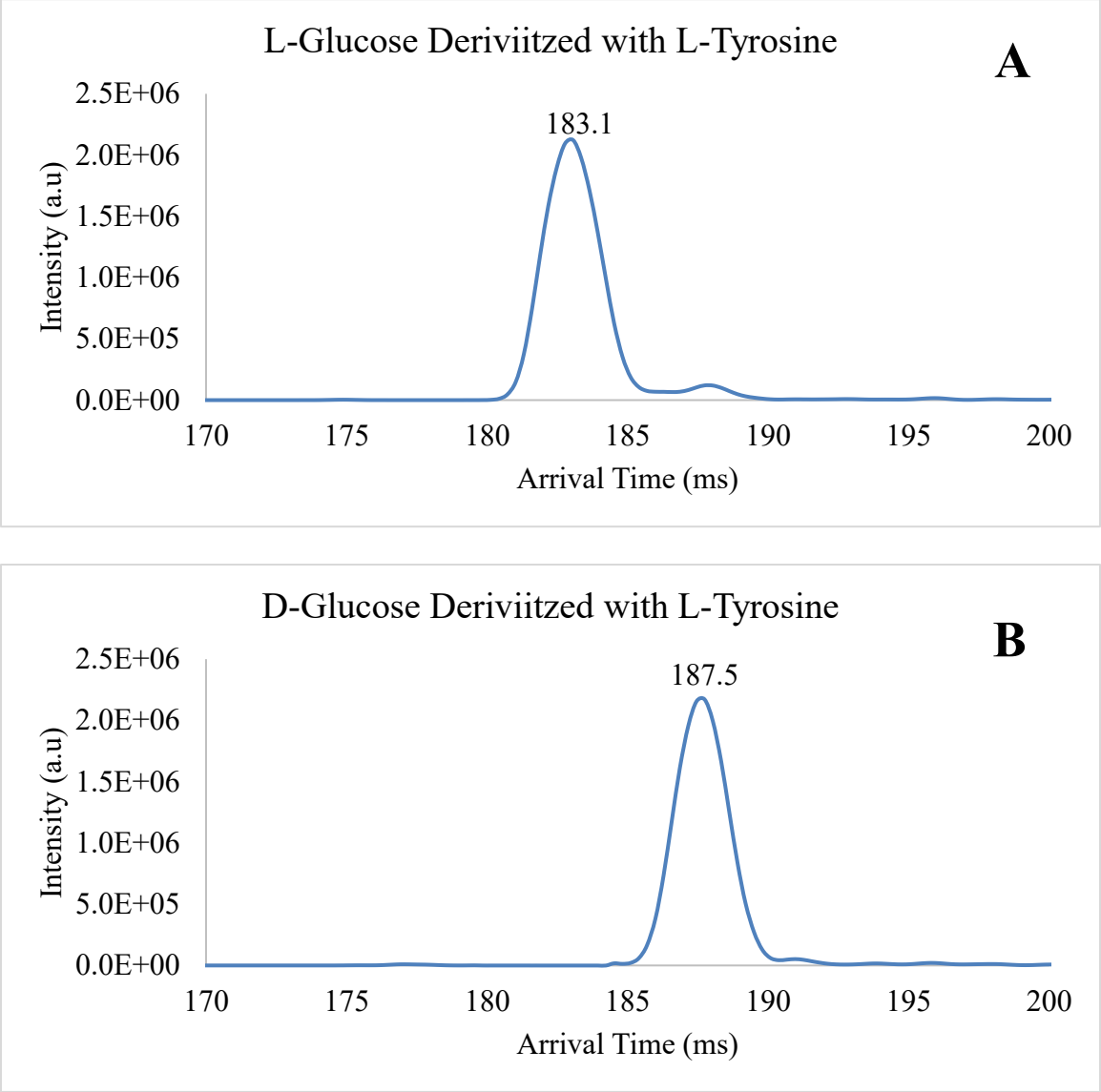

Figure 2.4 Displays the extracted mobiligram for 346. 13 $[M+H]^+$ for L- glucose (A) and D- glucose (B) derivatized with L-tyrosine.

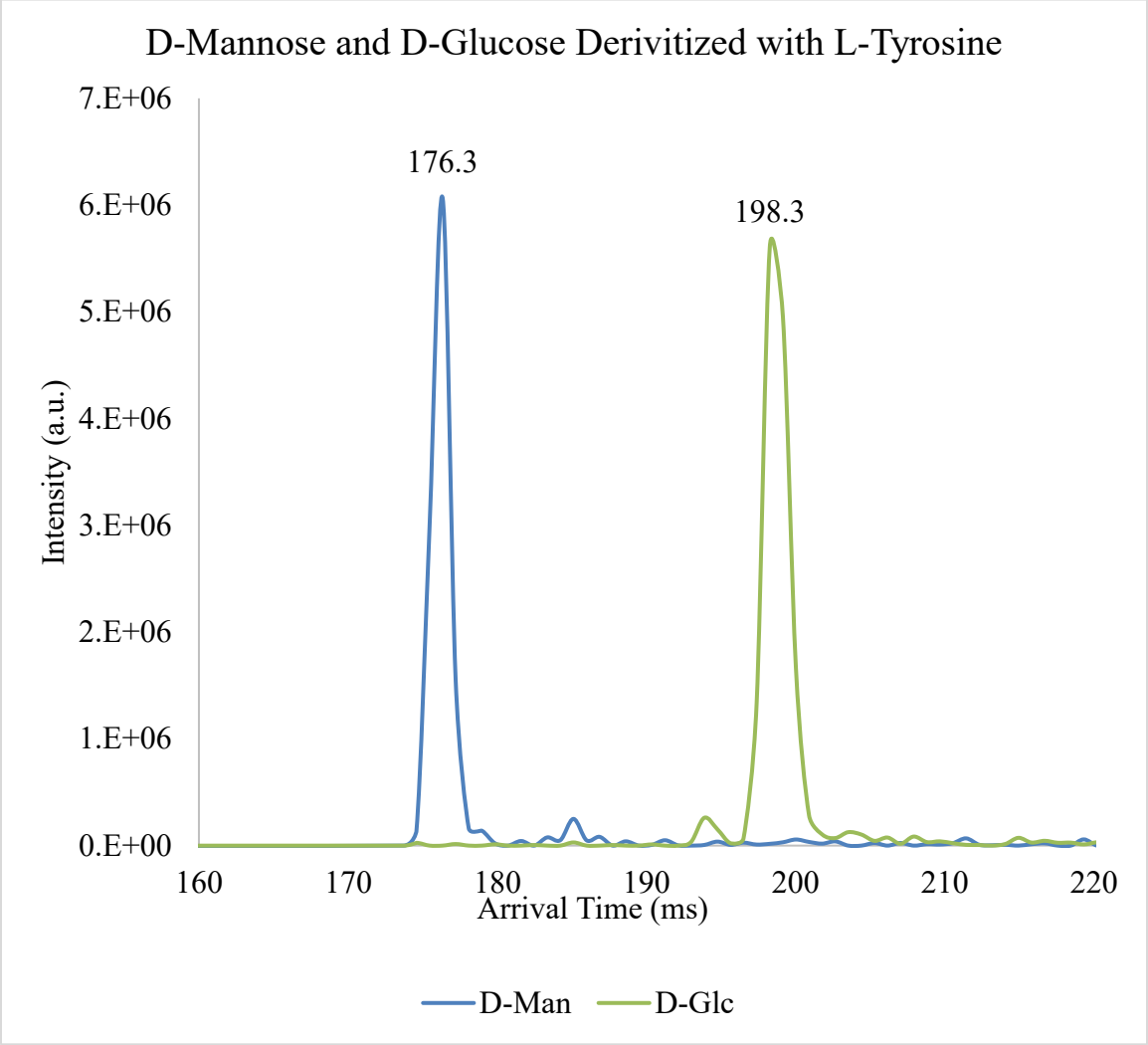

Figure 2.5 displays the extracted mobiligram for 346. 13 $[M+H]^+$ for D-mannose and D- glucose derivatized with L-tyrosine.

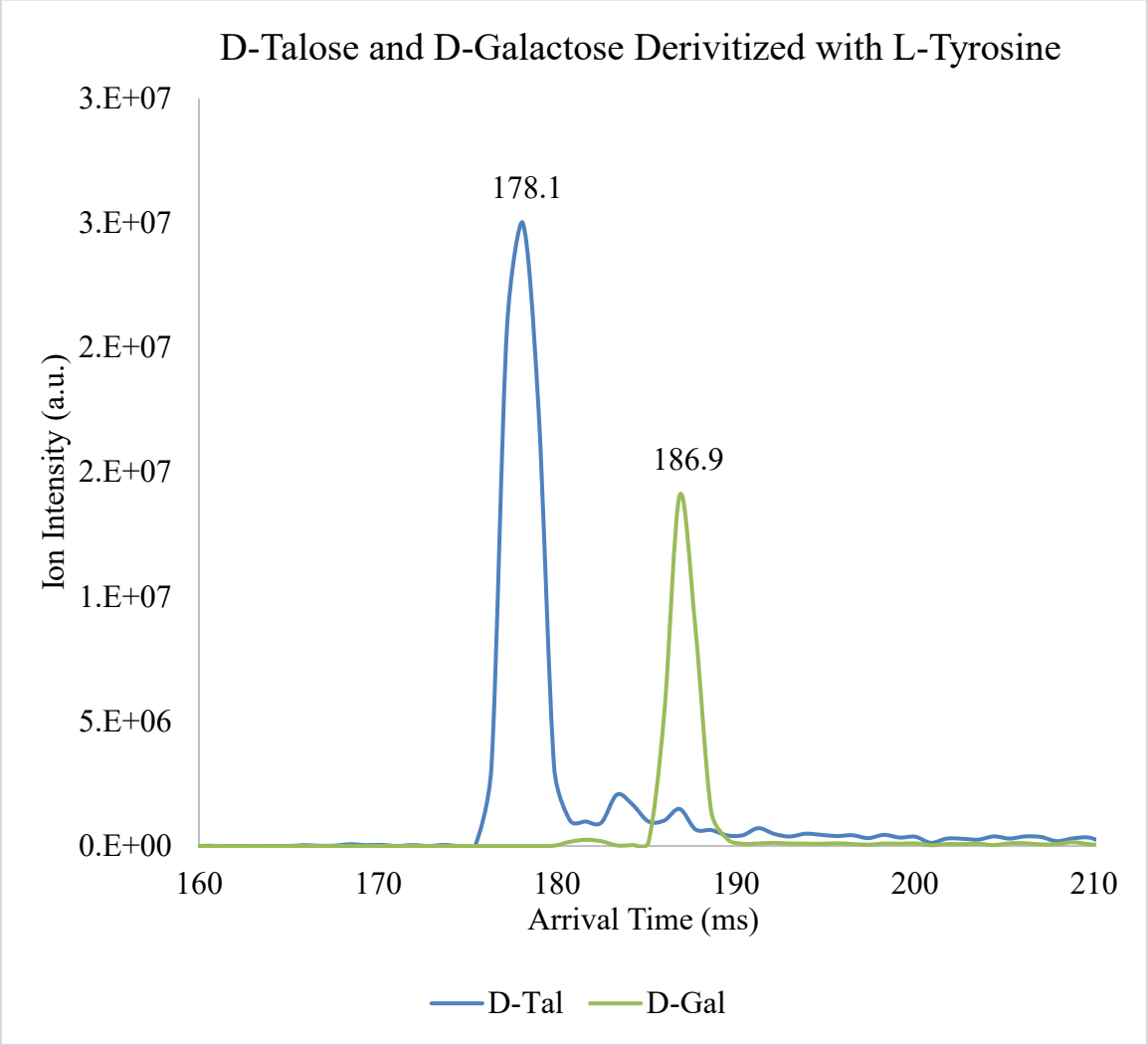

Figure 2.6 displays the extracted mobiligram for 346. 13 $[M+H]^+$ for D-mannose and D- glucose derivatized with L-tyrosine.

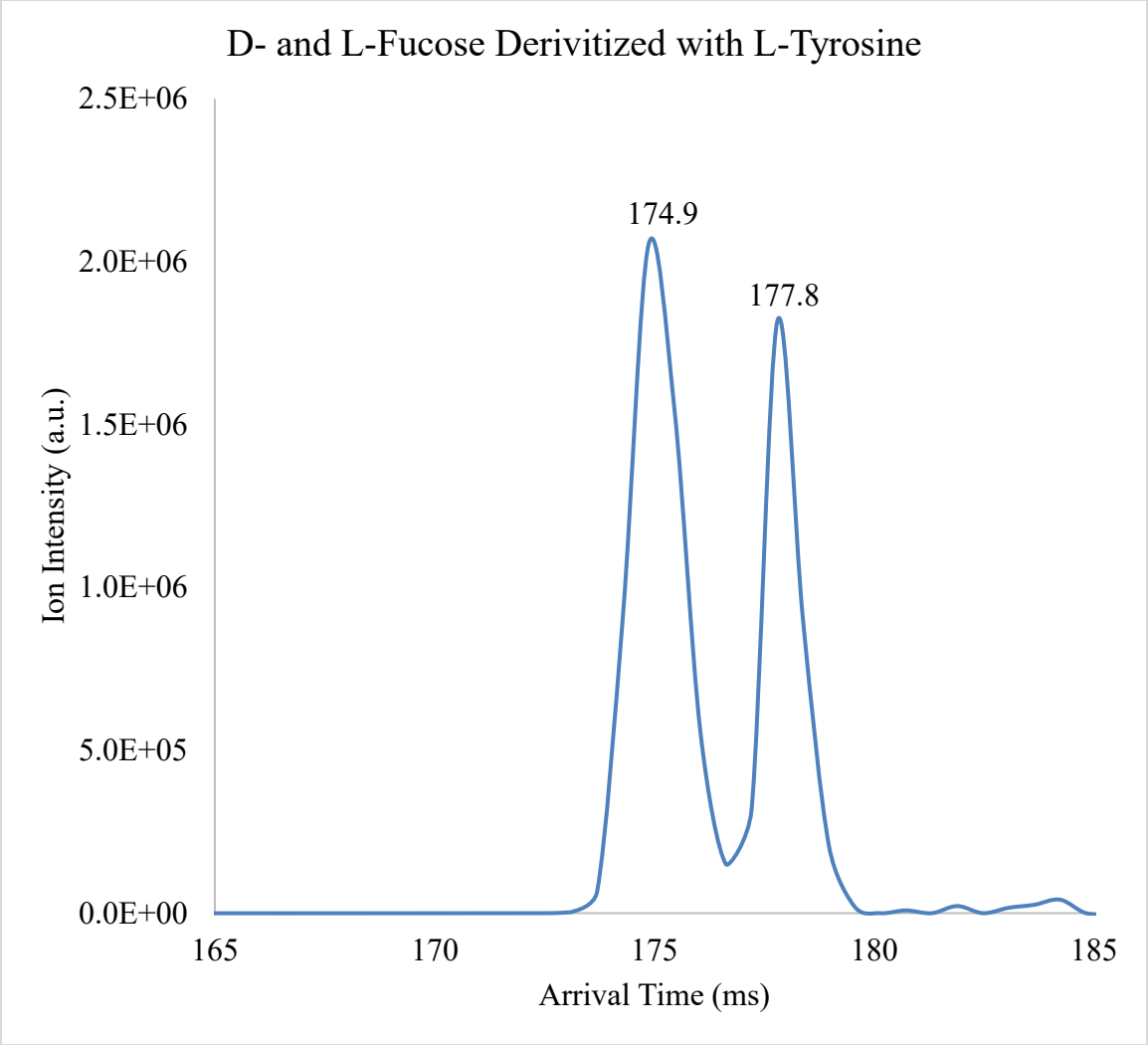

Figure 2.7. Extracted mobiligram of m/z 346.13 $[M+H]^+$ showing the separation of a mixture containing L-fucose and D-fucose derivatized with L-tyrosine.

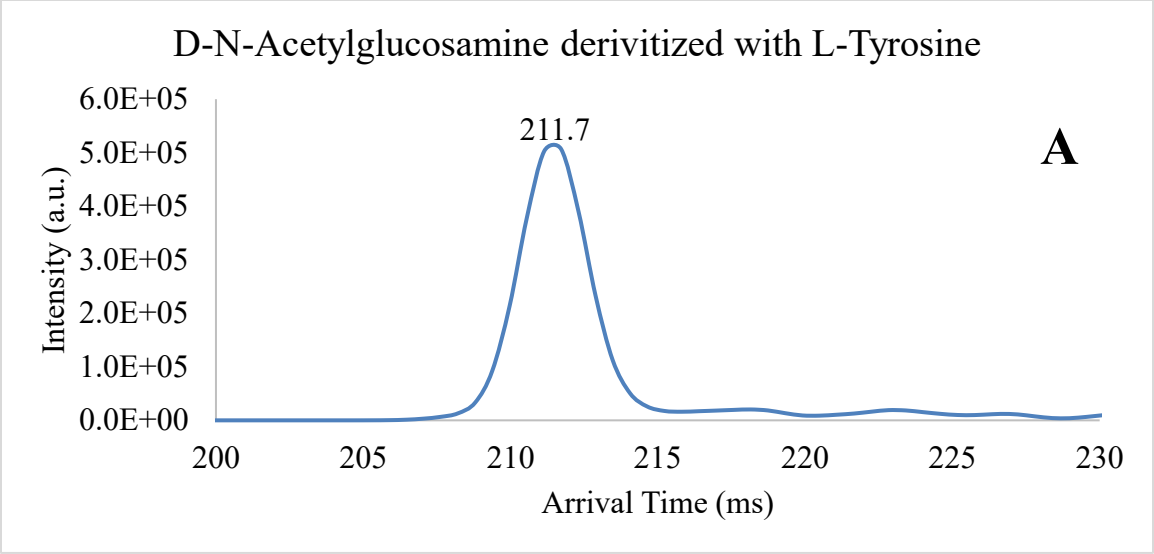

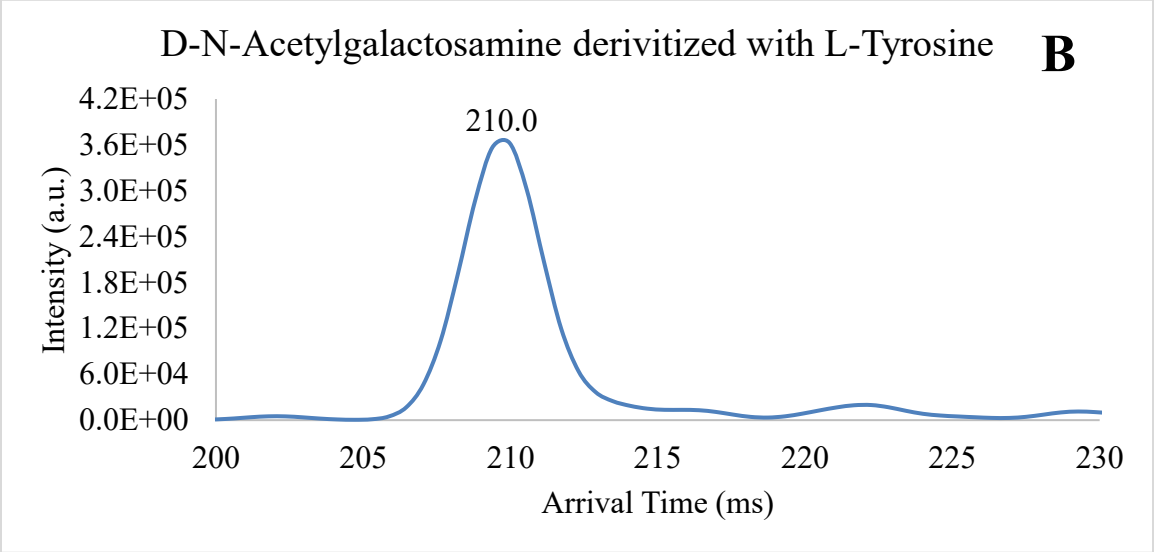

Figure 2.8 Displays the extracted mobiligram for 387.2 $[M+H]^+$ illustrating the separation of D-N-acetylglucosamine (A) and N-acetylgalactosamine (B) derivatized with L-tyrosine.

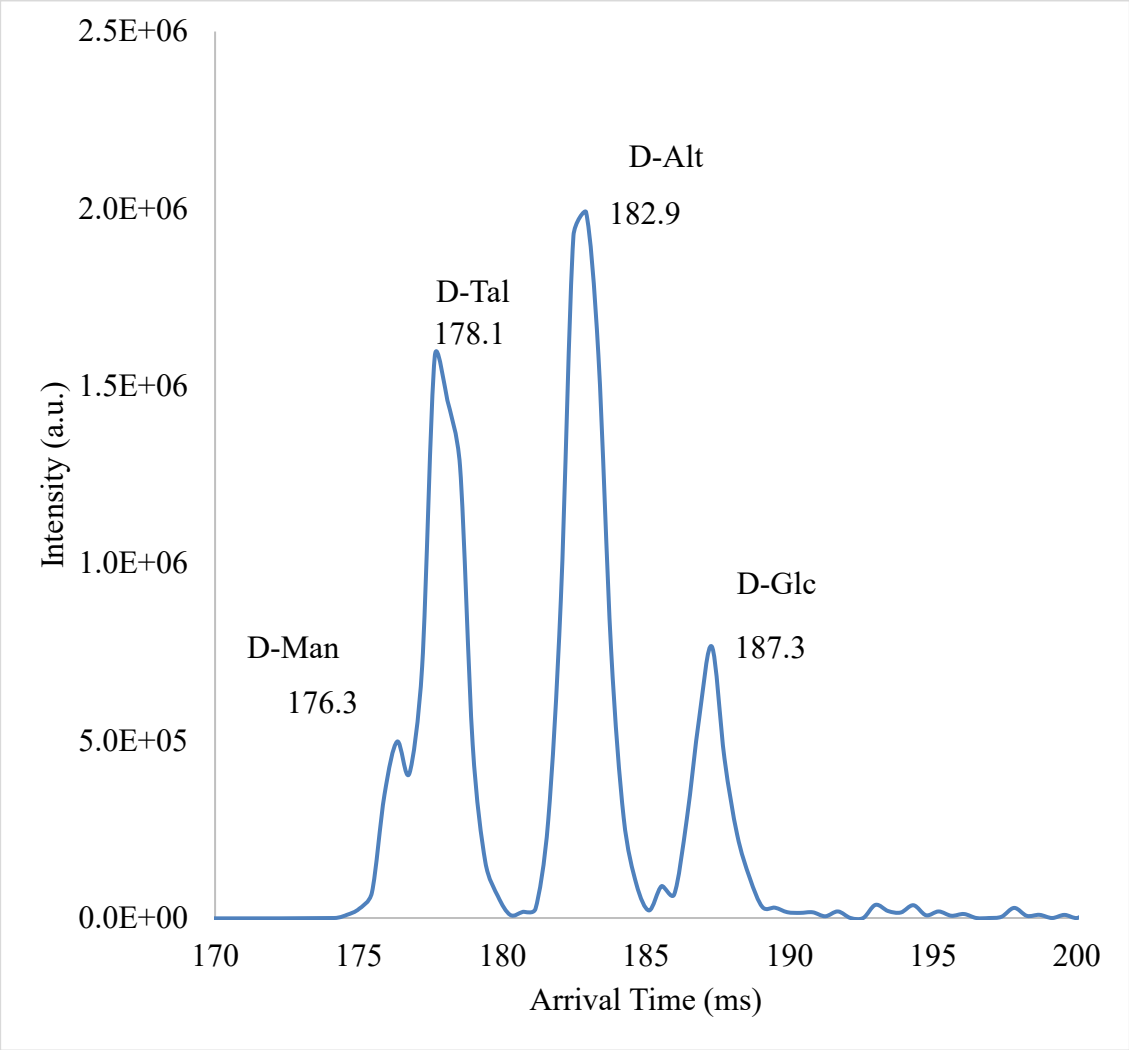

Figure 2.9 Displays the extracted mobiligram for 346. 13 $[M+H]^+$ for a set of standard monosaccharides (D-mannose, talose, altrose, and glucose) derivatized with L-tyrosine.

Hexose	Arrival Time (ms.)
D-Glucose	186.9
L-Glucose	182.5
D-Galactose	186.9
L-Galactose	181.6
D-Mannose	176.3
L-Mannose	185.1
D-Gulose	183.4
L-Gulose	172.0
D-Altrose	182.5
L-Altrose	187.7
D-Allose	177.2
L-Allose	183.4
D-Talose	183.4
L-Talose	177.2

Table 2.1 Arrival times (ms.) of aldohexose D and L enantiomers

References

1. Abdel-Magid, A. F., Carson, K. G., Harris, B. D., Maryanoff, C. A., & Shah, R. D. (1996a). Reductive Amination of Aldehydes and Ketones with Sodium Triacetoxyborohydride. Studies on Direct and Indirect Reductive Amination Procedures1. *The Journal of Organic Chemistry*, *61*(11), 3849–3862.
2. Abdel-Magid, A. F., Carson, K. G., Harris, B. D., Maryanoff, C. A., & Shah, R. D. (1996b). Reductive Amination of Aldehydes and Ketones with Sodium Triacetoxyborohydride. Studies on Direct and Indirect Reductive Amination Procedures1. *The Journal of Organic Chemistry*, *61*(11), 3849–3862.
3. Anumula, K. (1994). Quantitative Determination of Monosaccharides in Glycoproteins by High-Performance Liquid Chromatography with Highly Sensitive Fluorescence Detection. *Analytical Biochemistry*, *220*(2), 275–283.
4. Bawazeer, S., Ali, A. M., Alhawiti, A., Khalaf, A., Gibson, C., Tusiimire, J., & Watson, D. G. (2017). A method for the analysis of sugars in biological systems using reductive amination in combination with hydrophilic interaction chromatography and high-resolution mass spectrometry. *Talanta*, *166*, 75–80.
5. Habibi, S. C., Bradford, V. R., Baird, S. C., Lucas, S. W., Chouinard, C. D., & Nagy, G. (**2024**). Development of a cyclic ion mobility spectrometry-mass spectrometry-based collision cross-section database of permethylated human milk oligosaccharides. *Journal of Mass Spectrometry*, *59*(8).

6. Han, B., Park, J. W., Kang, M., Kim, B., Jeong, J., Kwon, O., & Son, J. (2020). Simultaneous analysis of monosaccharides using ultra high performance liquid chromatography-high resolution mass spectrometry without derivatization for validation of certified reference materials. *Journal of Chromatography B*, *1160*, 122370.
7. K, R., S, V. K., Saravanan, P., Rajeshkannan, R., Rajasimman, M., Kamyab, H., & Vasseghian, Y. (2023). Exploring the diverse applications of Carbohydrate macromolecules in food, pharmaceutical, and environmental technologies. *Environmental Research*, *240*, 117521.
8. Ma, J., Adler, L., Srzednicki, G., & Arcot, J. (**2016**). Quantitative determination of non-starch polysaccharides in foods using Gas Chromatography with flame ionization detection. *Food Chemistry*, *220*, 100–107.
9. Mayer, R. J., & Moran, J. (**2022**). Quantifying reductive amination in nonenzymatic amino acid synthesis. *Angewandte Chemie International Edition*, *61*(48).
10. Millette, P., Chabot, J., Sheppard, D. C., & Mauff, F. L. (**2023**). Identification and Quantification of Monosaccharides from Fungal Cell Walls and Exopolysaccharides by Gas Chromatography Coupled to Mass Spectrometry. *Current Protocols*, *3*(8).
11. Roy, R., Katzenellenbogen, E., & Jennings, H. J. (1984). Improved procedures for the conjugation of oligosaccharides to protein by reductive amination. *Canadian Journal of Biochemistry and Cell Biology*, *62*(5), 270–275.
12. Salehi, M., & Rashidinejad, A. (**2024a**). Multifaceted roles of plant-derived bioactive polysaccharides: A review of their biological functions, delivery, bioavailability, and

applications within the food and pharmaceutical sectors. *International Journal of Biological Macromolecules*, 138855.

13. Scholz, P., Chapman, K., Ischebeck, T., & Guzha, A. (**2023**). Analysis of Pectin-derived Monosaccharides. *BIO-PROTOCOL*, *13*(16).
14. Tang, W., Liu, D., & Nie, S. (**2022**). Food glycomics in food science: recent advances and future perspectives. *Current Opinion in Food Science*, *46*, 100850.
15. Veillon, L., Huang, Y., Peng, W., Dong, X., Cho, B. G., & Mechref, Y. (**2017a**). Characterization of isomeric glycan structures by LC-MS/MS. *Electrophoresis*, *38*(17), 2100–2114.
16. Wang, L., Xu, H., Yang, H., Zhou, J., Zhao, L., & Zhang, F. (**2022**). Glucose metabolism and glycosylation link the gut microbiota to autoimmune diseases. *Frontiers in Immunology*, *13*.
17. Willför, S., Pranovich, A., Tamminen, T., Puls, J., Laine, C., Suurnäkki, A., Saake, B., Uotila, K., Simolin, H., Hemming, J., & Holmbom, B. (**2008**). Carbohydrate analysis of plant materials with uronic acid-containing polysaccharides–A comparison between different hydrolysis and subsequent chromatographic analytical techniques. *Industrial Crops and Products*, *29*(2–3), 571–580.
18. Wu, H., Riggs, D. L., Lyon, Y. A., & Julian, R. R. (**2023**). Statistical framework for identifying differences in similar mass spectra: Expanding possibilities for isomer identification. *Analytical Chemistry*, *95*(17), 6996–7005.
19. Xu, B., Li, S., Ding, W., Zhang, C., Rehman, M. U., Tareen, M. F., Wang, L., & Huang, S. (2024). From structure to function: A comprehensive overview of polysaccharide roles and applications. *Food Frontiers*.

20. Zhang, Z., Khan, N. M., Nunez, K. M., Chess, E. K., & Szabo, C. M. (2012). Complete Monosaccharide Analysis by High-Performance Anion-Exchange Chromatography with Pulsed Amperometric Detection. *Analytical Chemistry*, *84*(9), 4104–4110.

CHAPTER 3

ENANTIOMER SEPARATION OF D- AND L- AMINO ACIDS BY ION MOBILITY-MASS SPECTROMETRY (IM-MS)

2 Brown, M., Orlando, R. To be submitted to a peer-reviewed journal

Abstract

Amino acids exist as enantiomers, with L- and D-forms sharing identical chemical structures but differing in biological activity. While L-amino acids are essential for protein synthesis, recent discoveries have revealed the physiological relevance of free D-amino acids in mammals. D-serine (D-Ser) and D-aspartic acid (D-Asp), for example, are present in mammalian tissues where they play key roles in neurotransmission, cell signaling, and age-related processes. Racemization of L- to D-amino acids occurs naturally over time, with D-Asp accumulation serving as a molecular marker of aging in tissues such as bone, arterial walls, and the brain. Therefore, distinguishing between D- and L-enantiomers whether in free form or embedded in peptides is crucial for understanding their functions in biological systems. This work provides as an analytical tool for enantiomer separation using reductive animation and ion mobility–mass spectrometry (IM-MS). Utilizing reductive animation converts enantiomers into diastereomers with carbohydrate tags. IM-MS analysis following derivatization enabled effective separation of most amino acid enantiomers and was further extended to evaluate enantiomeric composition within peptides.

Keywords: High resolution ion mobility–mass spectrometry, Amino Acids, Stereoisomers, Reductive amination, Chiral separation

Introduction

Amino acids are the essential building blocks of proteins and play critical roles in biological structure and function. Except for glycine, all amino acids are chiral and exist as two enantiomeric forms: L- and D-amino acids. These stereoisomers are non-superimposable mirror images that share identical chemical structures and physical properties such as solubility, polarity, and mass. However, they often differ significantly in biological function. While L-amino acids are predominantly used in protein biosynthesis, free D-amino acids have been identified in mammalian tissues and have recently gained attention for their physiological significance.

D-amino acids, such as D-serine (D-Ser) and D-aspartic acid (D-Asp), have been shown to participate in critical processes including neurotransmission, hormone regulation, and cellular signaling[1,2,3,4]. Their presence in the central nervous system and endocrine tissues suggests that these molecules may have broader roles than previously recognized. The conversion of L-amino acids into their D-enantiomers occurs through a process known as racemization[5], which takes place over time and is influenced by factors such as pH, temperature, and protein structure. Among the proteinogenic amino acids, aspartic acid is particularly prone to racemization[6], making D-Asp a well-studied marker of protein aging.

The accumulation of D-amino acids in long-lived tissues such as bone, cartilage, and brain have been linked to age-related diseases such as cataracts, atherosclerosis, and neurodegeneration[1]. As a result, accurate differentiation of amino acid enantiomers is essential for understanding their biological roles, monitoring tissue aging, and identifying potential biomarkers for disease. Despite their importance, distinguishing D- from L-

amino acids remains analytically challenging. Traditional techniques such as reversed-phase HPLC with chiral derivatization, capillary electrophoresis, and tandem mass spectrometry (MS/MS) have been used to resolve enantiomers[7]. However, these methods often involve complex derivatization protocols, limited sensitivity, or poor selectivity in complex biological matrices.

Reductive amination with optically active tags is a widely used strategy to convert enantiomers into diastereomers, enabling their separation by chromatographic or spectrometric means. However, the effectiveness of this approach is highly dependent on the chemical nature and position of the derivatization group. Additionally, many conventional workflows are time-intensive and not compatible with high-throughput analysis.

Ion mobility–mass spectrometry (IM-MS) offers an alternative strategy for stereoisomer resolution[8]. By separating ions in the gas phase based on their size, shape, and charge, IM-MS provides an orthogonal separation dimension to mass analysis. Coupling chiral derivatization with IM-MS enables the differentiation of structurally similar species, including amino acid enantiomers and diastereomeric peptides.

The objective of this study is to explore the application of reductive amination combined with IM-MS to resolve amino acid enantiomers and D-containing peptides. This method uses carbohydrate derivatization to convert enantiomers into structurally distinct diastereomers, enabling their separation by IM-MS. This approach aims to address the analytical challenges of enantiomer detection and provide an analytical tool for separating D-amino acids and peptide-bound forms.

Materials and Methods

Instrumentation and Separation Conditions

Experiments were performed using a high-resolution ion mobility (HRIM) MOBIE device (MOBILion Systems, Chadds Ford, PA, USA) coupled to an Agilent 6546 quadrupole time-of-flight (QTOF) mass spectrometer (Agilent Technologies, Santa Clara, CA, USA). Samples were ionized using the Agilent Dual Jet Stream Source (Dual AJS) in positive ionization mode. Mass spectrometer operation was controlled using Agilent MassHunter software (ver. B.0.9.0), while MOBILion's EyeOn software was used to control the SLIM system and acquire ion mobility data.

Sample introduction was carried out using an Agilent 1290 Infinity II LC stack (Agilent Technologies, Santa Clara, CA, USA). Separations were performed on a 1.5 × 150 mm HALO C-18-HILIC column packed with 2.7 μm superficially porous particles (Advanced Materials Technology, Wilmington, DE, USA). The column temperature was maintained at 60 °C, and the sample tray was held at ambient temperature. The mobile phases consisted of 10 mM ammonium formate in water with 0.1% formic acid (Solvent A) and 0.1% formic acid in acetonitrile (Solvent B). A linear gradient of 5% to 95% Solvent B was applied over 10 minutes at a flow rate of 0.1 mL/min. Injection volume was 5 μL, and the total run time, including column equilibration, was 20 minutes.

The SLIM device was operated at a chamber pressure of 2.5 Torr. Ions were accumulated in a designated trapping region and then released into the 13-meter serpentine separation pathway on the SLIM board. Traveling wave parameters were set to 15 kHz frequency and 30 V peak-to-peak (Vp-p) amplitude. Nitrogen gas was used for both drift and sheath gas, with flow rates of 9 L/min and 10 L/min, respectively. Source and sheath gas temperatures were 150 °C and 300 °C. The nebulizer pressure was set to

35 psi. Additional voltages included a fragmentor at 175 V, skimmer at 40 V, and octopole RF at 750 V. Data were acquired at a rate of 8 spectra/s, with 125 ms/spectrum across a mass range of 150–1700 m/z.

All LC-HRIM-MS data were recorded in .mbi format and converted to the Agilent .d format using MOBILion's HRIM Data Processor software (ver. 1.10.29.1). For enhanced signal clarity, data were processed using the PNNL Preprocessor software (ver. 4.0) with drift bin compression (2:1) and smoothing.

Chemicals and Samples

Carbohydrate standards including D-glucose, maltose, maltotriose, maltopentaose, and maltoheptaose were purchased from Sigma-Aldrich (St. Louis, MO, USA). L-glucose was purchased from Thermo Fisher Scientific (Waltham, MA, USA). D- and L-amino acids were purchased from Sigma-Aldrich. All peptides, including synthetic leucine enkephalin variants, were obtained from Abclonal Technology (Woburn, MA, USA). Reported purity of all carbohydrate, amino acid, and peptide standards ranged between 95–99%. HPLC-grade acetonitrile, water, and formic acid were purchased from Fisher Scientific (Hampton, NH, USA).

Reductive Amination Labeling Strategy

All amino acids and peptides were derivatized using carbohydrate tags via reductive amination. Derivatization of carbohydrates with Procainamide was performed as a precursor step, adapting protocols previously used for monosaccharide tagging. For labeling, 200 µL of a solution containing 0.4 M Procainamide HCl and 0.8 M sodium cyanoborohydride ($NaBH_3CN$) in dimethyl sulfoxide:acetic acid:water (7:2:1, v/v) was added to the carbohydrate and amino acid mixture. Samples were incubated at 65 °C

overnight. Following incubation, samples were dried using a vacuum centrifuge with no heat. The dried product was reconstituted in 240 μL of 5% acetic acid and cleaned using PD MiniTrap G10 desalting columns (Cytiva, Marlborough, MA, USA) following the manufacturer's protocol. Cleaned samples were dried again and resuspended in 100% water at a concentration of 1 mg/mL for LC-MS analysis. All solvents and chemicals were purchased from Fisher Scientific (Hampton, NH, USA).

Results/Discussion

This work evaluated the separation of D- and L-amino acid enantiomers using chiral derivatization with carbohydrates followed by ion mobility–mass spectrometry (IM-MS). Reductive amination was used to introduce carbohydrate tags, allowing the conversion of enantiomers into diastereomers with distinguishable gas-phase structures. This section discusses the derivatization strategy, the role of carbohydrate tag size on enantiomeric separation, and the extension of this approach to peptide-level stereochemistry.

Reductive Amination of Amino Acids

Reductive amination was used to derivatize amino acids with carbohydrates, enabling enantiomer separation by IM-MS. The reaction formed a Schiff base between the amino group of the amino acid and the reducing end of the sugar, followed by reduction to a stable secondary amine using sodium cyanoborohydride ($NaBH_3CN$). This transformation introduced a new chiral center at the C-1 position of the carbohydrate, converting enantiomers into diastereomers with distinct gas-phase conformations.

Initial evaluation was performed using glucose to derivatize D- and L-tyrosine. Ion mobility analysis demonstrated clear separation between the two isomers (Figure

3.1), confirming that this derivatization strategy could be extended to other amino acids. Derivatization of a broader panel of 19 amino acids (Table 3.1) using glucose revealed that several amino acids produced overlapping peaks in the mobiligram. Multiple peaks were observed for arginine and lysine due to the presence of secondary reactive amines, which contributed to lack of separation of enantiomers.

Selection of derivatization tag

Carbohydrate tag size was evaluated to improve resolution between enantiomers. Amino acids including alanine, leucine, arginine, tyrosine, and tryptophan were derivatized using maltose (disaccharide), maltotriose (trisaccharide), maltopentaose, and maltoheptaose. IM-MS results showed that increasing the size of the carbohydrate tag generally improved enantiomeric separation (Figure 3.2). Maltotriose derivatization yielded the best separation. Tags larger than three sugar units produced reduced resolution, likely due to increased diffusion and ion conformational flexibility, which impacted performance in the ion mobility cell.

Evaluation of tag size confirmed that amino acids with a large aromatic ring near the chiral center of the amino acid contributed to separation in the gas phase. However, exceeding an optimal size resulted in reduced performance, supporting the selection of maltotriose as the preferred tag for subsequent analyses.

Separation of Amino Acid Enantiomers by IM-MS

A set of 19 D- and L-amino acid pairs was derivatized with maltotriose and analyzed by IM-MS. Separation was observed for 14 of the 17 chiral amino acids (Figure 3.3). Amino acids such as glycine were excluded due to lack of chirality, while glutamine, methionine, and serine were not resolved. Arginine and lysine showed

multiple peaks and were excluded from further evaluation due to the presence of secondary reactive sites that interfered with signal interpretation. Results confirmed that the combination of reductive amination and IM-MS provided reliable separation for the majority of amino acid enantiomers. Conversion of enantiomers to diastereomers enhanced their gas-phase structural differences, enabling separation.

Peptide-Level Separation of D- and L-Forms

Peptides containing D-amino acids were evaluated to determine whether this derivatization approach could be extended beyond free amino acids. Leucine enkephalin, a pentapeptide containing three stereocenters, was used as a model. A comparison of native (L-form) and synthetic all-D peptide forms showed limited separation by IM-MS without derivatization (Figure 3.4). Following glucose tagging at the N-terminus through reductive amination, separation between the L- and D-peptides significantly improved (Figure 3.5). Site-specific D-substitutions were introduced at the tyrosine (N-terminal), phenylalanine (central), and leucine (C-terminal) residues to evaluate positional effects on separation. Substitution at the N-terminal tyrosine yielded the highest shift in arrival time (Figure 3.6), while substitution at the C-terminal leucine showed minimal separation (Figure 3.8). Substitution at the internal phenylalanine position resulted in intermediate separation efficiency (Figure 3.7). Data indicated that the proximity of the stereocenter to the derivatization site strongly influenced ion mobility separation. Separation was achieved when the D-amino acid was positioned closer to the derivatization tag, consistent with prior findings in small molecule isomer analysis.

Analytical Considerations and Outlook

Maltotriose derivatization in combination with IM-MS provided a rapid and reproducible method for enantiomer separation of amino acids and peptides. The success of this approach depended on tag size, stereocenter proximity to the tag, and the absence of interfering functional groups. While separation was not universally achieved across all amino acids, the method demonstrated clear advantages in throughput and structural sensitivity over traditional chromatographic techniques. Findings from this study establish a basis for future work applying this method to more complex peptide systems and biological mixtures. Incorporation of alternative derivatization reagents or functionalized tags may expand the scope of separable analytes and improve resolution for currently unresolved pairs.

Conclusion

This study demonstrated that D- and L-amino acid enantiomers can be separated using ion mobility–mass spectrometry (IM-MS) following derivatization with carbohydrate tags through reductive amination. The derivatization strategy converted enantiomers into diastereomers by introducing a chiral center at the C-1 position of the carbohydrate, enabling structural distinction in the gas phase. Evaluation of 19 amino acids revealed that 14 enantiomeric pairs were successfully separated using maltotriose as the derivatization tag. Tag size played a role in separation, with trisaccharides offering the greatest improvement in separation while maintaining ion mobility performance. Larger tags decreased separation efficiency, likely due to conformational flexibility and diffusion limitations. Application of this method to peptides confirmed that D- and L-forms could be resolved when a single D-amino acid was incorporated. Separation depended on the location of the D-substitution relative to the derivatization site.

Separation was achieved when the D-amino acid was positioned closer to the N-terminal tag, while epimers further down the sequence resulted in reduced separation. These results show a distance-dependent relationship between stereocenter position and gas-phase resolution. The results support the use of carbohydrate-based derivatization in combination with IM-MS as an analytical tool for the separation of amino acid enantiomers and site-specific peptide isomers. This approach offers a high-throughput alternative to traditional chromatographic techniques and holds promise for future applications in biological, clinical, and pharmaceutical research where chiral resolution is essential.

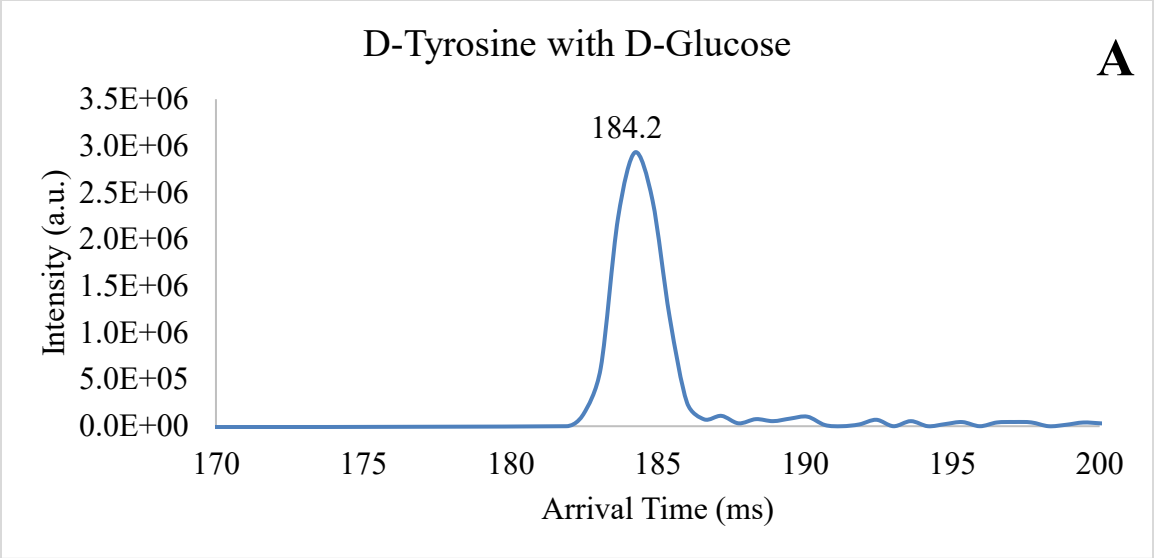

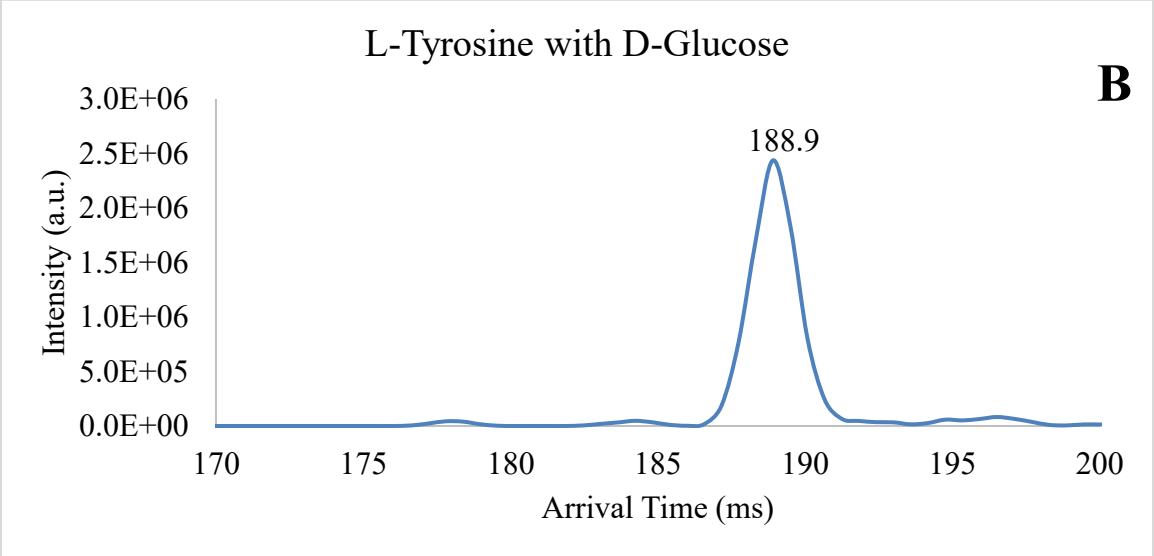

Figure 3.1 displays the extracted mobiligram for 346.13 $[M+H]^+$ for separation of L-(B) and D- (A) tyrosine derivatized with D-glucose

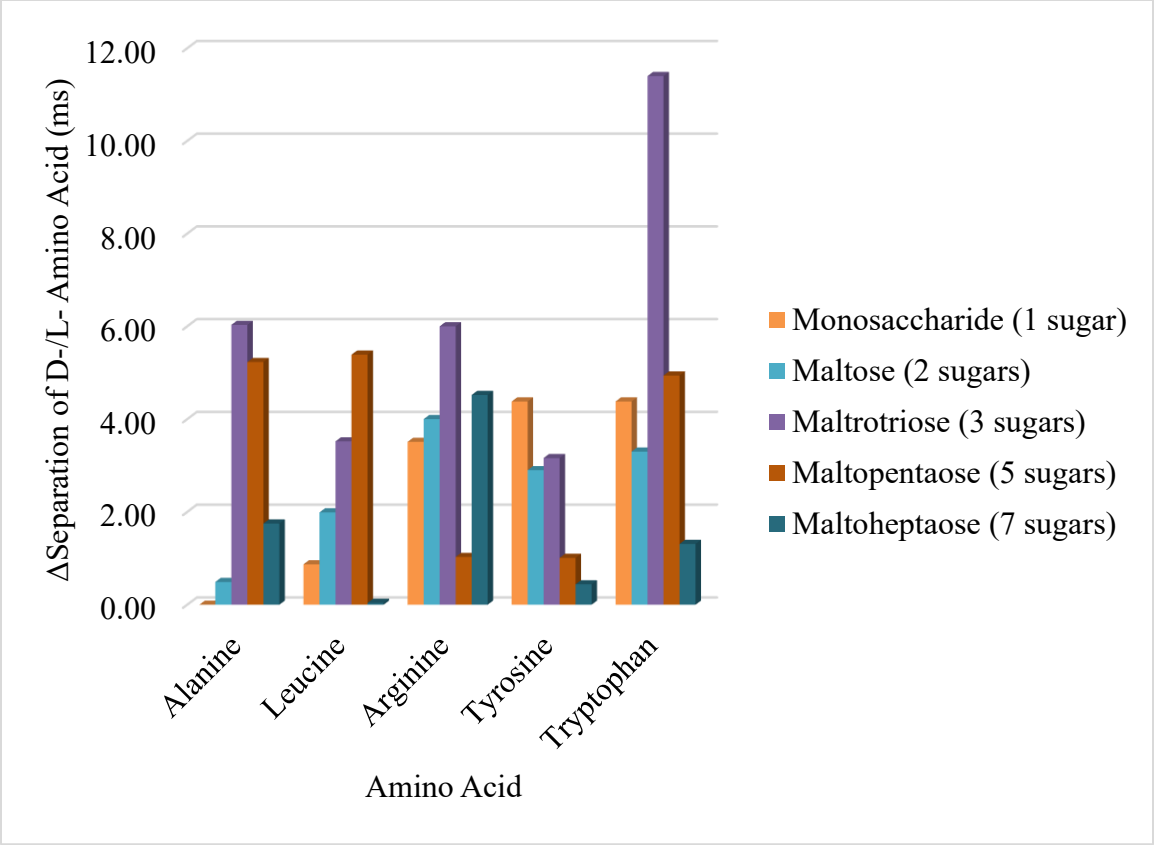

Figure 3.2 displays a table of the difference of separation between the D- and L-enantiomers of a few amino acids evaluated using different tags.

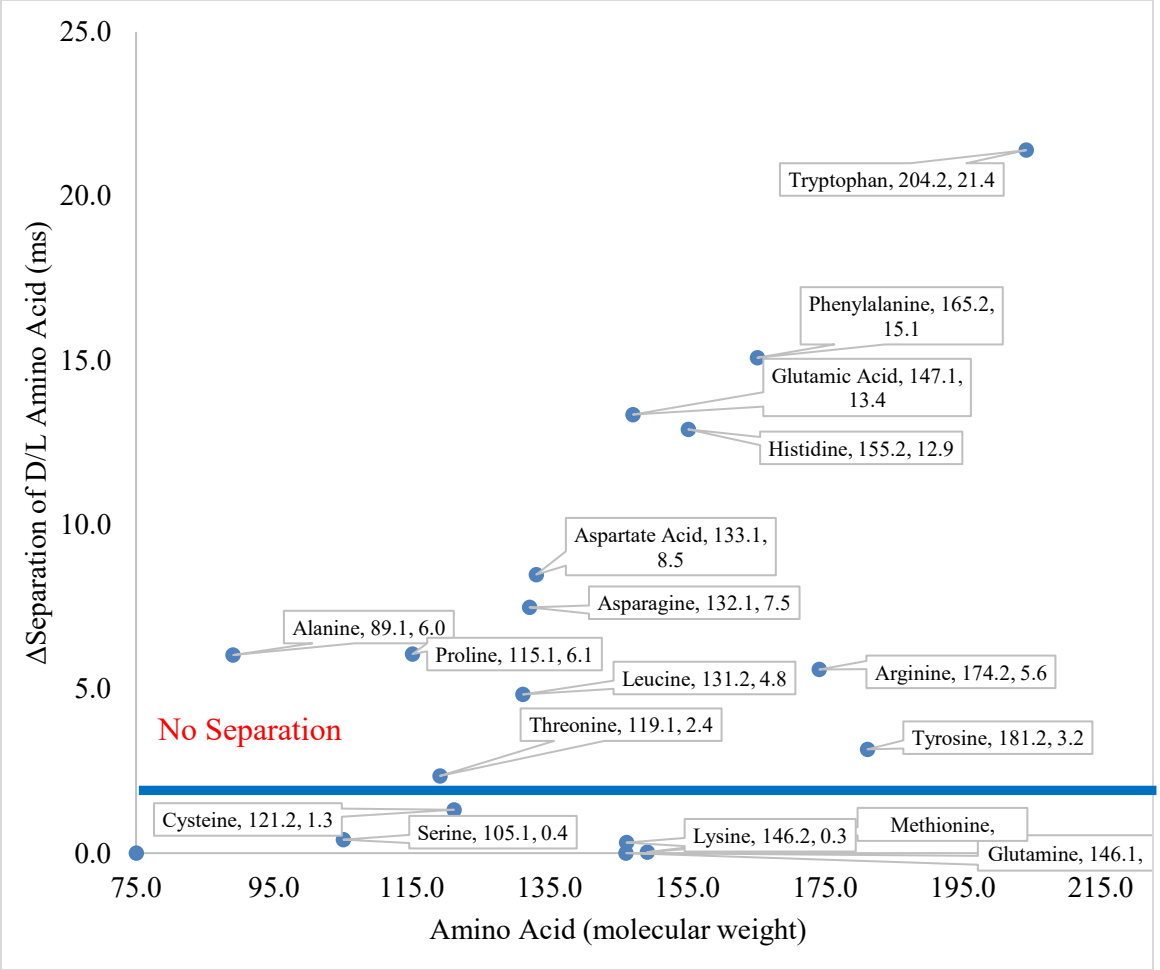

Figure 3.3 displays results from 17 D- and L- amino acids derivatized with maltrotriose.

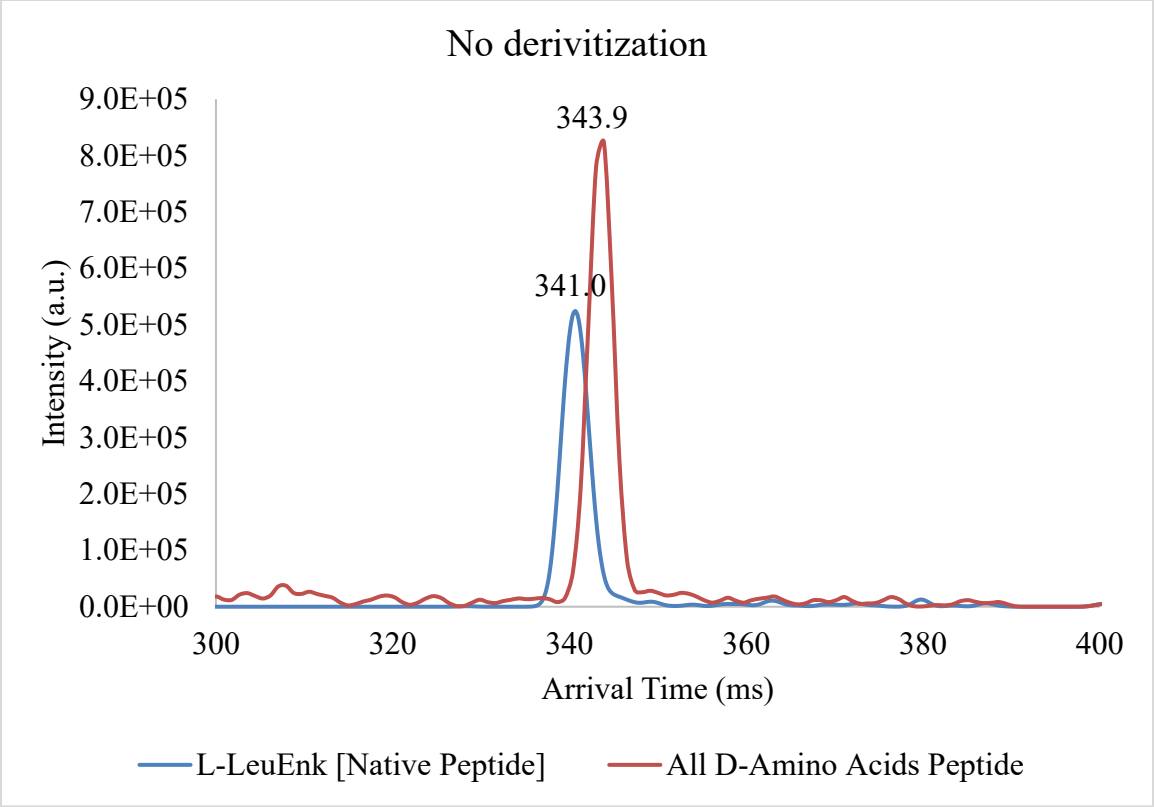

Figure 3.4 displays an extracted mobiligram for the native L-amino acid containing peptide and the synthetic peptide with all D-amino acids.

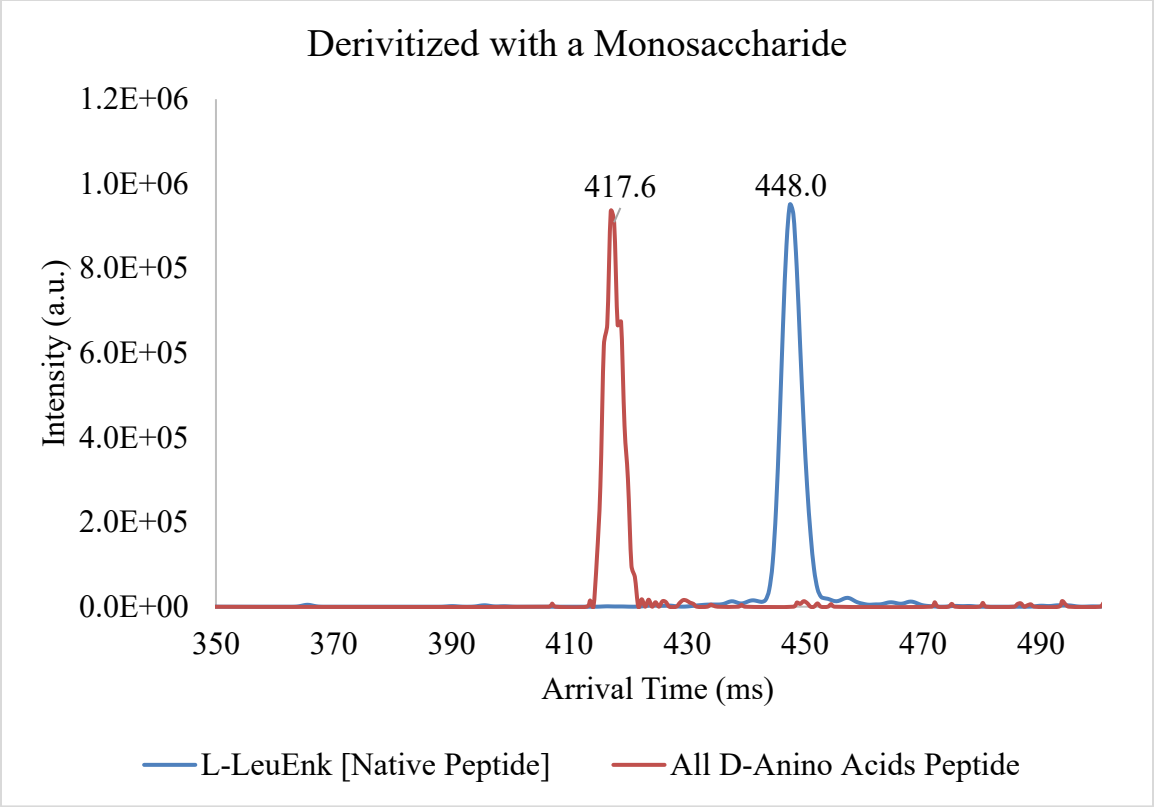

Figure 3.5 displays an extracted mobiligram for the native L-amino acid containing peptide and the synthetic peptide with all D-amino acids derivatized with d-glucose.

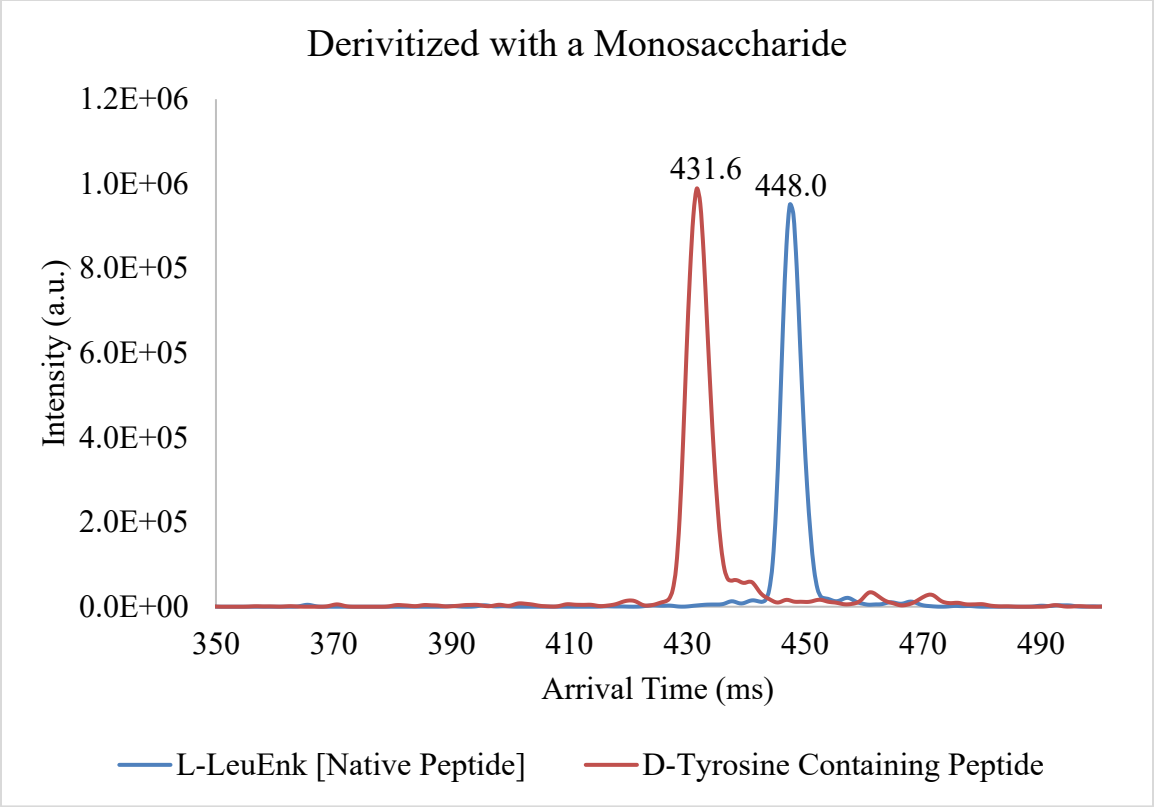

Figure 3.6 displays an extracted mobiligram for leucine enkephalin derivatives with D-glucose at the n-terminus.

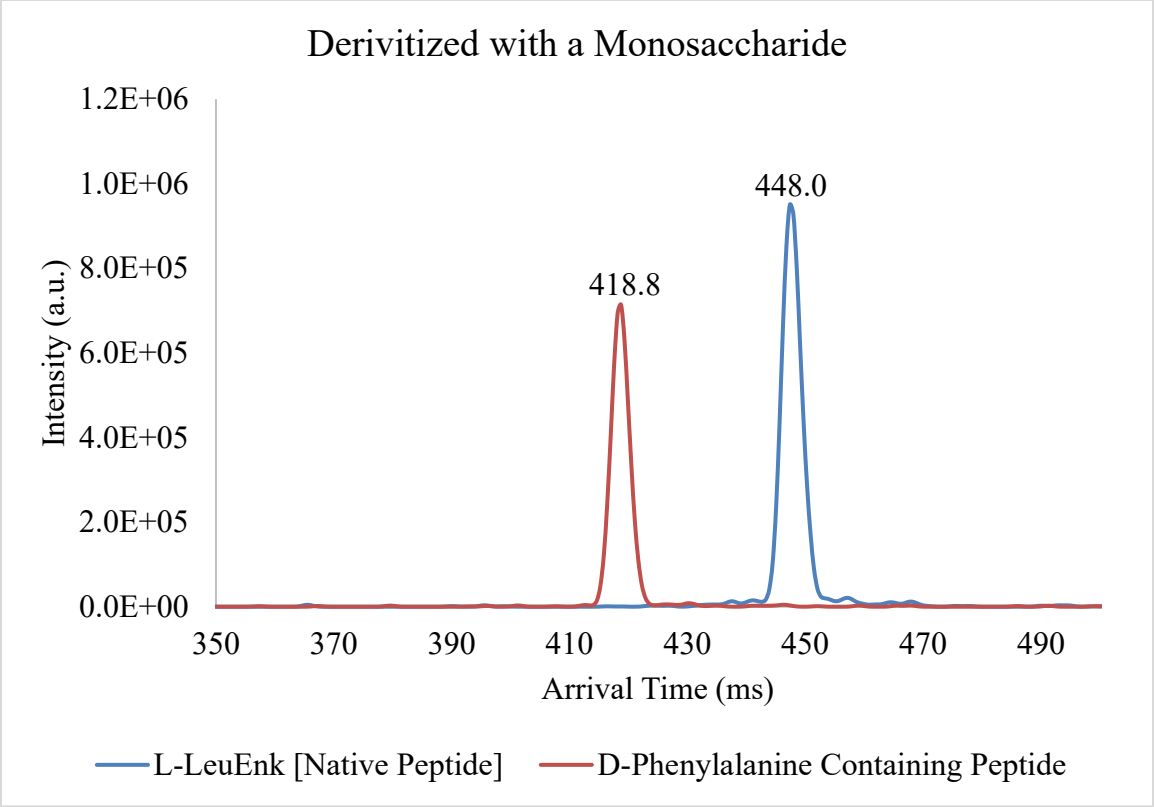

Figure 3.7 displays an extracted mobiligram for leucine enkephalin derivatives with D-glucose at the n-terminus.

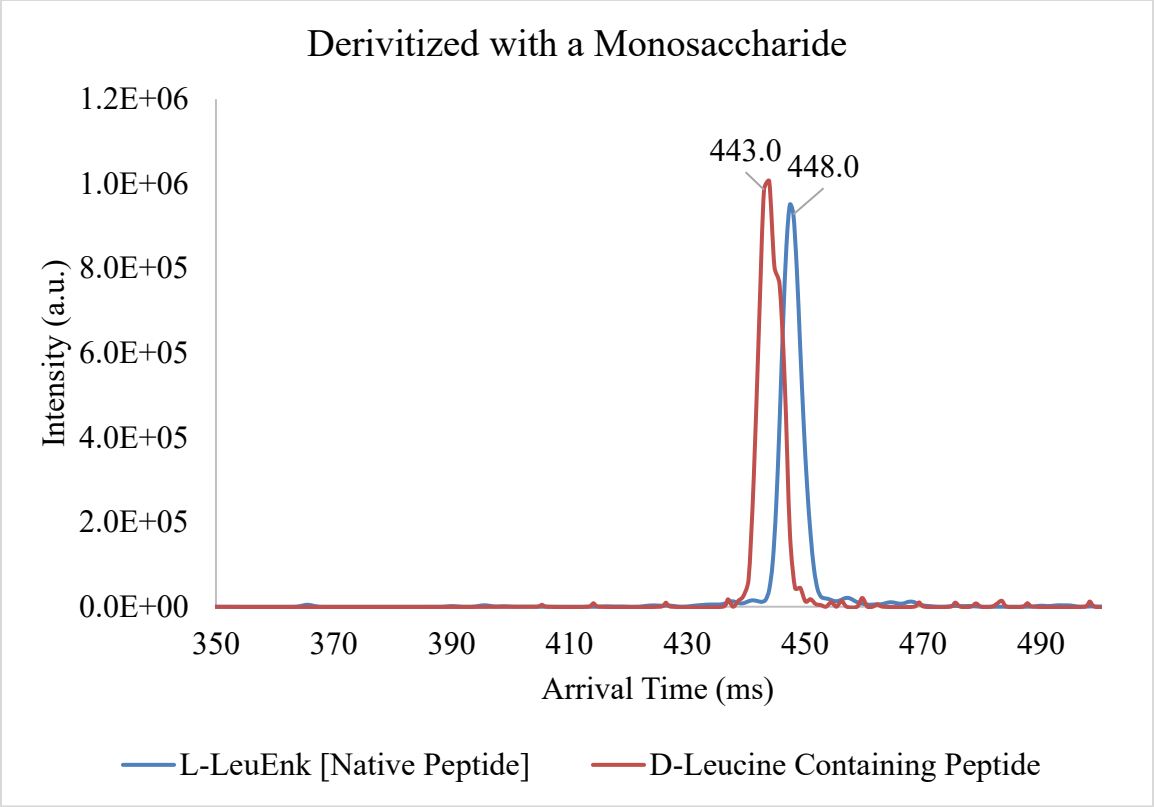

Figure 3.8 displays an extracted mobiligram for leucine enkephalin derivatives with D-glucose at the n-terminus.

Amino Acid	Arrival Time (ms)	M/Z	Amino Acid	Arrival Time (ms)	M/Z
D-Glycine	308.14	240.1 $[M+H]^+$	L-Glycine	308.14	240.1 $[M+H]^+$
D-Alanine	322.69	254.1 $[M+H]^+$	L-Alanine	316.66	254.1 $[M+H]^+$
D-Serine	317.04	270.1 $[M+H]^+$	L-Serine	316.63	270.1 $[M+H]^+$
D-Proline	323.73	280.1 $[M+H]^+$	L-Proline	329.79	280.1 $[M+H]^+$
D-Threonine	334.01	284.1 $[M+H]^+$	L-Threonine	336.36	284.1 $[M+H]^+$
D-Cysteine	341.56	286.1 $[M+H]^+$	L-Cysteine	340.24	286.1 $[M+H]^+$
D-Leucine	367.08	296.2 $[M+H]^+$	L-Leucine	362.25	296.2 $[M+H]^+$
D-Isoleucine	155.25	296.2 $[M+H]^+$	L-Isoleucine	156.12	296.2 $[M+H]^+$
D-Asparagine	333.7	297.1 $[M+H]^+$	L-Asparagine	326.22	297.1 $[M+H]^+$
D-Aspartate Acid	334.17	298.1 $[M+H]^+$	L-Aspartate Acid	325.69	298.1 $[M+H]^+$
D-Glutamine	368.00	311.1 $[M+H]^+$	L-Glutamine	355.45	311.1 $[M+H]^+$
D-Lysine	514.80	311.2 $[M+H]^+$	L-Lysine	515.12	311.2 $[M+H]^+$
D-Glutamic Acid	367.55	312.1 $[M+H]^+$	L-Glutamic Acid	354.20	312.1 $[M+H]^+$
D-Methionine	400.97	314.1 $[M+H]^+$	L-Methionine	400.94	314.1 $[M+H]^+$
D-Histidine	361.79	320.1 $[M+H]^+$	L-Histidine	348.89	320.1 $[M+H]^+$
D-Phenylalanine	360.49	330.1 $[M+H]^+$	L-Phenylalanine	375.57	330.1 $[M+H]^+$
D-Arginine	377.23	339.2 $[M+H]^+$	L-Arginine	382.82	339.2 $[M+H]^+$
D-Tyrosine	376.56	346.2 $[M+H]^+$	L-Tyrosine	373.40	346.2 $[M+H]^+$
D-Tryptophan	393.99	369.1 $[M+H]^+$	L-Tryptophan	372.59	369.1 $[M+H]^+$

Table 3.1 Arrival times (ms) and m/z of D- and L-amino acids derivatized with a monosaccharide (d-glucose) by IM-MS.

References

1. Bastings, J. J. A. J., van Eijk, H. M., Olde Damink, S. W., & Rensen, S. S. (2019). d-amino Acids in Health and Disease: A Focus on Cancer. Nutrients, 11(9), 2205.
2. Zapico, S., & Ubelaker, D. H. (2022). Application of Aspartic Acid Racemization for Age Estimation in a Spanish Sample. Biology, 11(6), 856.,
3. Desiderio, C., & Aturki, Z. (1997). Enantiomeric resolution study by capillary electrophoresis. Journal of Chromatography A, 772(1-2), 185–194.
4. McCudden, C. R., & Kraus, V. B. (2006). Biochemistry of amino acid racemization and clinical application to musculoskeletal disease. Clinical Biochemistry, 39(12), 1112–1130.
5. Ota, N., Shi, T., & Sweedler, J. V. (2012). d-Aspartate acts as a signaling molecule in nervous and neuroendocrine systems. Amino Acids, 43(5), 1873–1886.
6. Wolosker, H. (2017). The Neurobiology of d -Serine Signaling. Advances in Pharmacology, 82, 325–348.
7. Wolosker, H., Dumin, E., Balan, L., & Foltyn, V. N. (2008). d-Amino acids in the brain: d-serine in neurotransmission and neurodegeneration. FEBS Journal, 275(14), 3514–3526.
8. Wu, Q., Wang, J.-Y., Han, D.-Q., & Yao, Z.-P. (2020). Recent advances in differentiation of isomers by ion mobility mass spectrometry. TrAC Trends in Analytical Chemistry, 124, 115801–115801.

9. Abdulbagi, M., Wang, L., Siddig, O., Di, B., & Li, B. (2021). D-Amino Acids and D-Amino Acid-Containing Peptides: Potential Disease Biomarkers and Therapeutic Targets? *Biomolecules*, *11*(11), 1716.
10. Asbury, G. R., & Hill, H. H. (1999). Using Different Drift Gases To Change Separation Factors (α) in Ion Mobility Spectrometry. *Analytical Chemistry*, *72*(3), 580–584.
11. Bastings, J. J. A. J., van Eijk, H. M., Olde Damink, S. W., & Rensen, S. S. (2019). d-amino Acids in Health and Disease: A Focus on Cancer. *Nutrients*, *11*(9), 2205.
12. Bhatia, S., & Randhir Dahiya. (2015). Plant-Based Biotechnological Products With Their Production Host, Modes of Delivery Systems, and Stability Testing. *Elsevier EBooks*, 293–331.
13. Bhushan, R., & Bruckner, H. (2004). Marfey's reagent for chiral amino acid analysis: A review. *Amino Acids*, *27*(3-4), 231–247
14. Bizzotto, E., Zampieri, G., Treu, L., Filannino, P., Raffaella Di Cagno, & Campanaro, S. (2024). Classification of bioactive peptides: A systematic benchmark of models and encodings. *Computational and Structural Biotechnology Journal*, *23*, 2442–2452.
15. Cava, F., Lam, H., de Pedro, M. A., & Waldor, M. K. (2011). Emerging knowledge of regulatory roles of D-amino acids in bacteria. *Cellular and Molecular Life Sciences: CMLS*, *68*(5), 817–831.
16. Chernobrovkin, M. G., Anan'eva, I. A., Shapovalova, E. N., & Shpigun, O. A. (2004). Determination of Amino Acid Enantiomers in Pharmaceuticals by Reversed-Phase High-Performance Liquid Chromatography. *Journal of Analytical Chemistry*, *59*(1), 55–63.

17. Fujii, N., Kaji, Y., & Fujii, N. (2011). d-Amino acids in aged proteins: Analysis and biological relevance. *Journal of Chromatography B*, *879*(29), 3141–3147.

18. Fujii, N., Takata, T., Fujii, N., Aki, K., & Sakaue, H. (2018). D-Amino acids in protein: The mirror of life as a molecular index of aging. *Biochimica et Biophysica Acta (BBA) - Proteins and Proteomics*, *1866*(7), 840–847

19. Grishin, D. V., Zhdanov, D. D., Pokrovskaya, M. V., & Sokolov, N. N. (2019). D-amino acids in nature, agriculture, and biomedicine. *All Life*, *13*(1), 11–22.

20. Grün, R. (2008). AMINO ACID RACEMIZATION DATING. *Encyclopedia of Archaeology*, 429–433.

21. Ha, S., Kim, I., Takata, T., Kinouchi, T., Isoyama, M., Suzuki, M., & Fujii, N. (2017). Identification of D-amino acid-containing peptides in human serum. *PLOS ONE*, *12*(12), e0189972.

22. Kaji, Y., Oshika, T., Takazawa, Y., Fukayama, M., Takata, T., & Fujii, N. (2007). Localization of D-β-Aspartic Acid–Containing Proteins in Human Eyes. *Investigative Opthalmology & Visual Science*, *48*(9), 3923.

23. Kalidasan, V., Suresh, D., Zulkifle, N., Hwei, Y. S., Kok Hoong, L., Rajasuriar, R., & Theva Das, K. (2024). Investigating D-Amino Acid Oxidase Expression and Interaction Network Analyses in Pathways Associated With Cellular Stress: Implications in the Biology of Aging. *Bioinformatics and Biology Insights*, *18*.

24. Kiriyama, Y., & Nochi, H. (2016). D-Amino Acids in the Nervous and Endocrine Systems. *Scientifica*, *2016*(6494621), 1–9.

25. Larriba-Andaluz, C., & Carbone, F. (2021). The size-mobility relationship of ions, aerosols, and other charged particle matter. *Journal of Aerosol Science*, *151*, 105659–105659.

26. Masumi Katane, & Homma, H. (2024). Biosynthesis and Degradation of Free D-Amino Acids and Their Physiological Roles in the Periphery and Endocrine Glands. *Biological & Pharmaceutical Bulletin*, *47*(3), 562–579.

27. Morvan, M., & Mikšík, I. (2021). Recent Advances in Chiral Analysis of Proteins and Peptides. *Separations*, *8*(8), 112.

28. Müller, C., Fonseca, J. R., Rock, T. M., Krauss-Etschmann, S., & Schmitt-Kopplin, P. (2014). Enantioseparation and selective detection of D-amino acids by ultra-high-performance liquid chromatography/mass spectrometry in analysis of complex biological samples. *Journal of Chromatography A*, *1324*, 109–114.

29. Nasyrova, R. F., Khasanova, A. K., Altynbekov, K. S., Asadullin, A. R., Markina, E. A., Gayduk, A. J., Shipulin, G. A., Petrova, M. M., & Shnayder, N. A. (2022). The Role of D-Serine and D-Aspartate in the Pathogenesis and Therapy of Treatment-Resistant Schizophrenia. *Nutrients*, *14*(23), 5142.

30. Sulaiman Al-Sulaimi, Reveka Kushwah, Al-Sibani, M., Atef El Jery, Moutaz Aldrdery, & Ghulam Abbas Ashraf. (2023). Emerging Developments in Separation Techniques and Analysis of Chiral Pharmaceuticals. *Molecules*, *28*(17), 6175–6175.

31. Truscott, R. J. W. (2010). Are Ancient Proteins Responsible for the Age-Related Decline in Health and Fitness? *Rejuvenation Research*, *13*(1), 83–89.

32. Vantomme, G., & Crassous, J. (2021). Pasteur and chirality: A story of how serendipity favors the prepared minds. *Chirality*, *33*(10), 597–601.

CHAPTER 4

ADVANCING HILIC RETENTION MODELING: CAN A RETENTION MODEL FOR N-GLYCANS BE DEVELOPED THAT APPLIES TO MULTIPLE STATIONARY PHASES?

3 Brown, M., Orlando, R. To be submitted to a peer-reviewed journal

Abstract:

N-linked glycosylation is an important post-translational modification. Characterization of N-glycans are often analyzed by hydrophilic interaction liquid chromatography (HILIC)-MS after tagging with a fluorophore. While mass spectrometry (MS) can provide broad identification of N-glycans, distinguishing between isomeric and isobaric structures requires refined methods. HILIC retention times can give structural information not obtained by MS when an unknown retention time is compared to a database of standards. This approach works for structures that have been previously identified but fails for glycans not found in the database. The aim of this study is to develop a method to predict the retention time for all N-glycans on various stationary phases, expanding the analysis to glycans not included in the database.

Keywords: Hydrophilic Interaction Liquid Chromatography (HILIC), N-Linked Glycans, Mass Spectrometry, Glycan Analysis, Retention Time Prediction

Introduction

Glycosylation is a common post-translational modification that occurs in the endoplasmic reticulum (ER) and plays a crucial role in protein folding, stability, and function[10,24]. It involves the attachment of carbohydrate (glycan) to specific amino acid residues and can be classified into two types: N-linked and O-linked glycosylation. N-linked glycans are covalently attached to the nitrogen atom of asparagine residues, typically within a consensus sequence motif Asn-X-Ser/Thr (where X is any amino acid except proline)[1]. In contrast, O-linked glycans are linked to the hydroxyl groups of serine or threonine residues[4]. These glycan structures are essential in determining protein function, localization, and biological activity[8]. Given the biological roles of glycans, it is essential to understand their structure and diversity.

Structural characterization of glycans are often performed using mass spectrometry[9,15] due to their high sensitivity and ability to distinguish species with identical masses. Analytical approaches focus on either glycopeptide analysis or the study of released glycans, and sensitivity can be enhanced by fluorescent derivatization strategies[17]. Analytical strategies typically focus on either glycans that have been enzymatically released from glycoproteins or glycopeptides generated through proteolytic digestion. While glycopeptide analysis provides site-specific information[6], analysis of released glycans offers detailed compositional profiling[19] and insights into isomeric variation which is key for understanding structure function relationships.

To distinguish closely related glycan isomers, liquid chromatography (LC) is often coupled with mass spectrometry (MS), enabling both separation and structural elucidation. In a typical workflow, N-glycans are enzymatically released from

glycoproteins and may be derivatized with a fluorescent tag such as 2-aminobenzamide (2-AB), 2-aminobenzoic acid, or procainamide[13,18] to enhance detection and improve chromatographic behavior. These labeled glycans are then separated by LC before being introduced into the mass spectrometer. Among the different modes of LC separation, hydrophilic interaction liquid chromatography (HILIC) is effective for glycan separations due to the highly polar nature of carbohydrate structures. HILIC enables resolution of isomeric species based on differences in polarity and branching but also provides consistent retention behavior that can be linked to glycan structure[4,12].

Previous work have shown that the addition of individual monosaccharide units, such as hexoses, N-acetylhexosamine, or sialic acids, results in shifts in retention time shifts[9], allowing additional information for the identification of structural features. This shows how retention time models can be utilized which aim to predict glycan behavior based on structural attributes and improve the confidence of glycan identification.

However, relying solely on retention time databases presents limitations in accurately determining structures. These databases are typically built from a restricted set of glycan structures, leading to limited coverage and difficulty identifying novel or uncommon glycans. Additionally, retention times are often column- and method-specific, making inter-laboratory comparisons challenging. When a glycan is not present in the database, accurate identification may be difficult or impossible. Even when a match exists, false positives and ambiguous identifications can occur specifically for isomeric or isobaric species.

In this study, the aim is to evaluate if a linear regression based model can predict retention times for N-glycans using multiple HILIC stationary phases and derivatization

tags. This approach will focus on broadening the analytical capabilities of HILIC-MS for comprehensive glycan characterization.

Material / Methods

N-Glycan release

N-glycans were released from glycoprotein standards, including transferrin (human), fetuin (bovine), and RNaseB (bovine). Erythropoietin-FC fusion (CHO) acquired from GlycoScientific (Athens, GA, USA). Protein samples were suspended in 50mM Ammonium Bicarbonate (1ug/ul) and reduced by adding 5uL of 200 mM dithiothreitol (DTT) and placed in the heat block at 65^{c} for 1 hour. Followed by adding 5uL of 1 M iodoacetamide (IDA) (sample was left in a dark location for 1 hour at room temperature) to prevent the reformation of disulfide bonds. To deactivate the IDA, samples were incubated in the heat block at 65^{c} for 1 hour with 20uL of 200 mM dithiothreitol (DTT). The sample was dried using the speed vacuum with no heat and resuspend in 50mM Ammonium Bicarbonate at a concentration of 1 ug/uL where 2-4uL of PNGaseF (Lectenz Bio, Athens, GA, USA)were added followed by incubating the sample at 37^{c} overnight. Released glycans were then purified from the protein by drying the sample down in speed vac. 200 µL of 5% acetic acid was added and the sample was sonicated for 10-15 min before performing glycan purification. C18 cartridge (ThermoScientific, Rockwood, TN, USA) were washed with 3 mL MeOH and equilibrated with 3 mL 5% acetic acid. Sample was loaded onto the column. N-glycans were eluted with 4 mL of 5% acetic acid as glycans do not retain on a C18 column (ThermoScientific, Rockwood, TN, USA) . Sample was then dried using speed vacuum and labeled via reductive amination.

All solvents and reagents were purchased from Sigma-Aldrich (St. Louis, MO, USA) unless otherwise specified.

Labeling Released Glycans with Reductive amination

Samples were tagged with a variety of fluorophores, such as 2-aminobenzoic acid (2-AA), 2-aminobenzamide (2-AB), and Procainamide (ProA). Labeling was performed with sodium cyanoborohydride (NaBH3CN) reductive amination. 60 µL of 0.4 M Procainamide HCl (Sigma Aldrich, St. Louis, MO, USA), 0.8 M NaBH3CN (Sigma Aldrich, St. Louis, MO, USA) was added to this part, mixed in dimethyl sulfoxide :acetic acid;7:3 (v/v) and incubated at 65°C overnight. All fluorophores followed this same procedure. Samples were then dried using speed vacuum. Then the sample was resuspended in 5% acetic acid (240µL) and cleaned on a PD MiniTrap G10 desalting column (Cytiva, Marlborough, MA, USA) using the manufacturer's protocol. The samples were then dried and resuspended in 100% Milli-Q water (1 mg/mL) for LC-MS analysis.

LC-MS Instrument Settings

LC separations were performed on both neutral and zwitterionic stationary phases. Neutral separations were achieved using the penta-HILIC phase (Advanced Materials Technology, Wilmington, DE, USA), while zwitterionic separations were performed on both Zic-cHILIC and Zic-HILIC phases (Millipore Sigma, Bellefonte, PA,USA). Experiments were conducted using the Nexera UFLC (Shimadzu, Kyoto, Kyoto, Japan) coupled with the Synapt G2Si Q-TOF (Waters, Milford, MA, USA). A linear gradient of 80–40% B over 40 minutes at a flow rate of 0.200 mL/min was used for generating coefficients for model. Model evaluation was conducted on an optimized

separation method using a 70–30% B gradient over 20 minutes at 0.400 mL/min. Peak areas were determined using Skyline, and multivariable linear regression analysis was performed in Excel.

Results/Discussion

A linear regression model was used to create HILIC RT coefficients for evaluation across different HILIC stationary phases. The model was created in glucose units (GU) to allow for comparability between different LC methods. Following by evaluating the accuracy of the model by comparing calculated RT values to experimental values.

Retention Time Model

Previous work[13] has demonstrated the potential of retention time (RT) prediction models for N-linked glycan analysis using a neutral penta-HILIC stationary phases. The model was developed from a dataset of N-linked glycan signals, and overall, the neutral hydrophilic character of Penta-HILIC provided useful structural information for glycan identification. However, when applied to other stationary phases, the derived coefficients from Penta-HILIC were not sufficient for accurate predictions, highlighting the need for alternative approaches.

To address this, a similar approach was followed and expanded by using multiple stationary phases. New coefficients were generated for the three LC stationary phase with different surface modifications. All of the coefficients are expressed in glucose units (GU) to allow for transferability to other LC–MS system. To calculate the RT of a glycan the sum of each retention motif is determined by its experimentally derived coefficient.

$$R = \sum N_x M_x$$

N_x: the number of a particular monosaccharide x present in the glycan of interest

M_x: the coefficient of Retention motif

The model was generated by taking a collection of N-glycans released from Fetuin, RNase B, Transferrin, and Erythropoietin-Fc. All glycans were analyzed by LC-MS using two HILIC zwitterionic columns (Zic-HILIC and Zic-cHILIC) in triplicate. A linear regression analysis was performed by considering each retention subunit from RT to glucose units. From this analysis a model was created that statically considered the relationship between a dependent variable (retention time in GU) and the independent variables (each retention altering subunit).

Development of Coefficients

To generate coefficients, glycoprotein standards were enzymatically deglycosylated and labeled via reductive amination with fluorescent tags. Samples were analyzed by LC-MS using a shallow gradient (80–40% B over 40 minutes), collecting MS1 data. Data interpretation was performed manually, assisted by Skyline (Figure 4.1), and glycan structures were confirmed with literature references. This approach was repeated in triplicate across all three stationary phases (Penta-HILIC, Zic-HILIC, and Zic-cHILIC) in Figure 4.1, 4.2, and 4.3. After data collection, all observed glycan structures were compiled and sorted based on their monosaccharide composition and chromatographically resolved linkages. A table was generated in Excel listing 49 distinct chromatographic structures. Duplicate structures observed from multiple glycoproteins were noted but not treated as new. The retention times (in minutes) for all structures were recorded, and correlations between retention-altering subunits and RTs were established.

The resulting model yielded coefficients for each retention motif (Table 4.1). The coefficients for hexose and HexNAc were very similar, suggesting comparable retention effects across all three stationary phases. Notably, the neutral Penta-HILIC column exhibited the largest retention coefficient, indicating that hydrogen bonding plays a greater role in retention on this phase compared to the mixed mode zwitterionic phases. This supports Dr. Andrew Alpert's proposed mechanism involving a water layer in HILIC separations[1]. Charged motifs such as sialic acid α2-3 and α2-6 showed the greatest variability across stationary phases. As previously reported, alpha 2-3 sialic acids eluted earlier[15] than alpha 2-6 on all columns. On the Zic-HILIC phase, which features a sulfobetaine group with overall neutral charge but weak ionic interactions, a smaller coefficient was observed which is likely due to charge repulsion[2]. Conversely, the Zic-cHILIC column showed increased retention for sialic acids, potentially due to protonation effects[12,15]. Coefficients on the zwitterionic phases were generally smaller than those on the neutral Penta-HILIC.

Evaluation of RT Model

The model's accuracy was assessed by comparing calculated RT values to experimental RTs, averaging across three replicates. Data was then assessed by calculating a percent deviation by taking the difference between the experimental and calculated RT and dividing them by the experimental RT. This metric was used to account for differences in glycan retention across various stationary phases. For simplicity, the analysis described will focus on the results from fetuin glycans. The neutral column showed an average deviation between experimental and calculated retention times for the n-glycans were 0.02 minutes with the largest deviation being 0.06

minutes (Figure 4.4). Retention time predictions on the negatively charged ZIC-HILIC column showed an average deviation of 0.03 minutes between experimental and calculated values; the maximum deviation observed was 0.08 minutes (Figure 4.5). Retention time predictions on the positively charged ZIC-cHILIC column showed an average deviation of 0.01 minutes and a maximum deviation of 0.04 minutes between experimental and calculated values (Figure 4.6). These results demonstrate the model's robustness across different stationary phases and highlight its potential for predicting RTs on different stationary phases. An example of how the model can predict retention is shown in Figure 4.7 with EPO-Fc, using the zic-cHILIC. This demonstrates how the model can be applied to different LC conditions. This data was run on a faster gradient which shows the transferability of the model when using glucose units instead of RT in minutes.

Conclusion

These results show how tailoring monosaccharide coefficients to specific HILIC stationary phases improves retention time prediction accuracy. By summing these retention motif coefficients, the model reliably predicted the RTs of N-glycans across both neutral and zwitterionic HILIC phases. This can be applied for glycans not included in model training set as well as using different labels (tags) for the released n-glycans. Importantly, this approach remained effective even when LC conditions varied, demonstrating the model's robustness and its potential to provide complementary structural information to MS data.

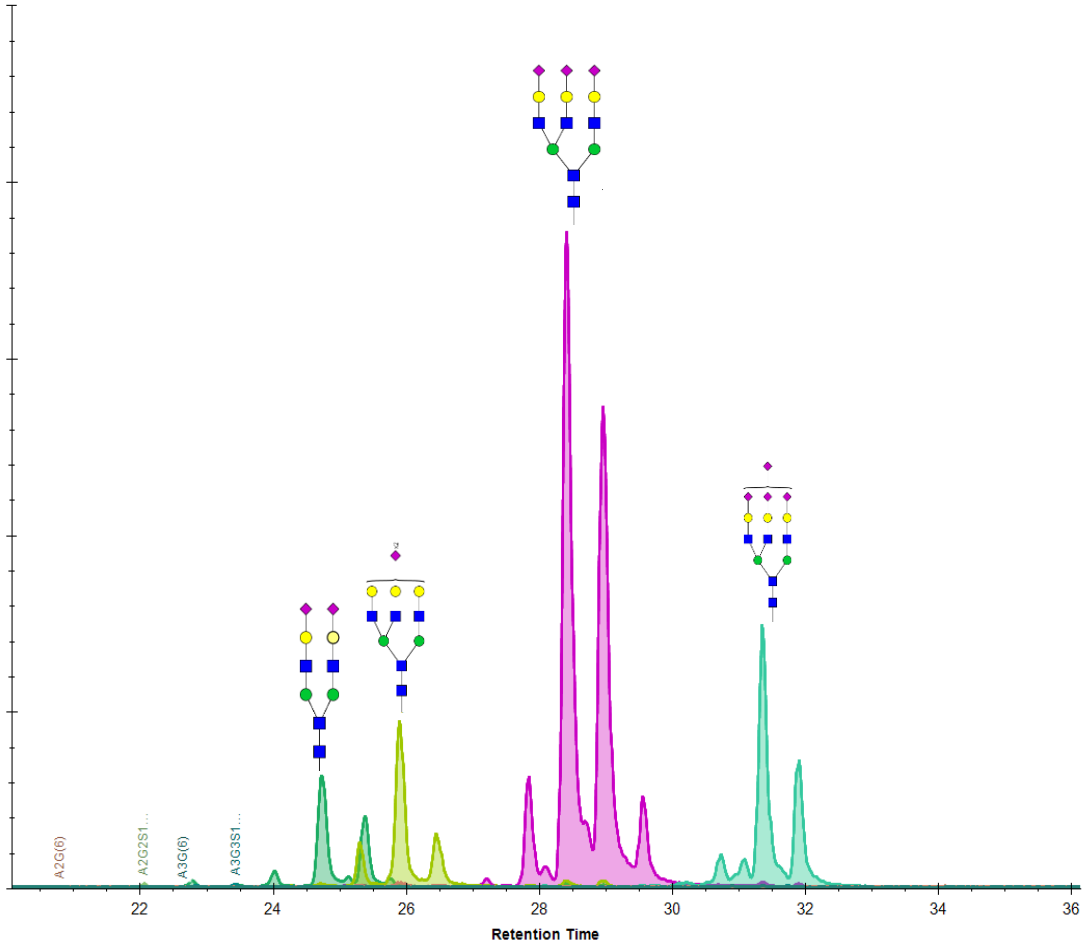

Figure 4.1 Chromatographic separation of isomeric and linkage-specific N-glycans on the neutral Penta-HILIC column.

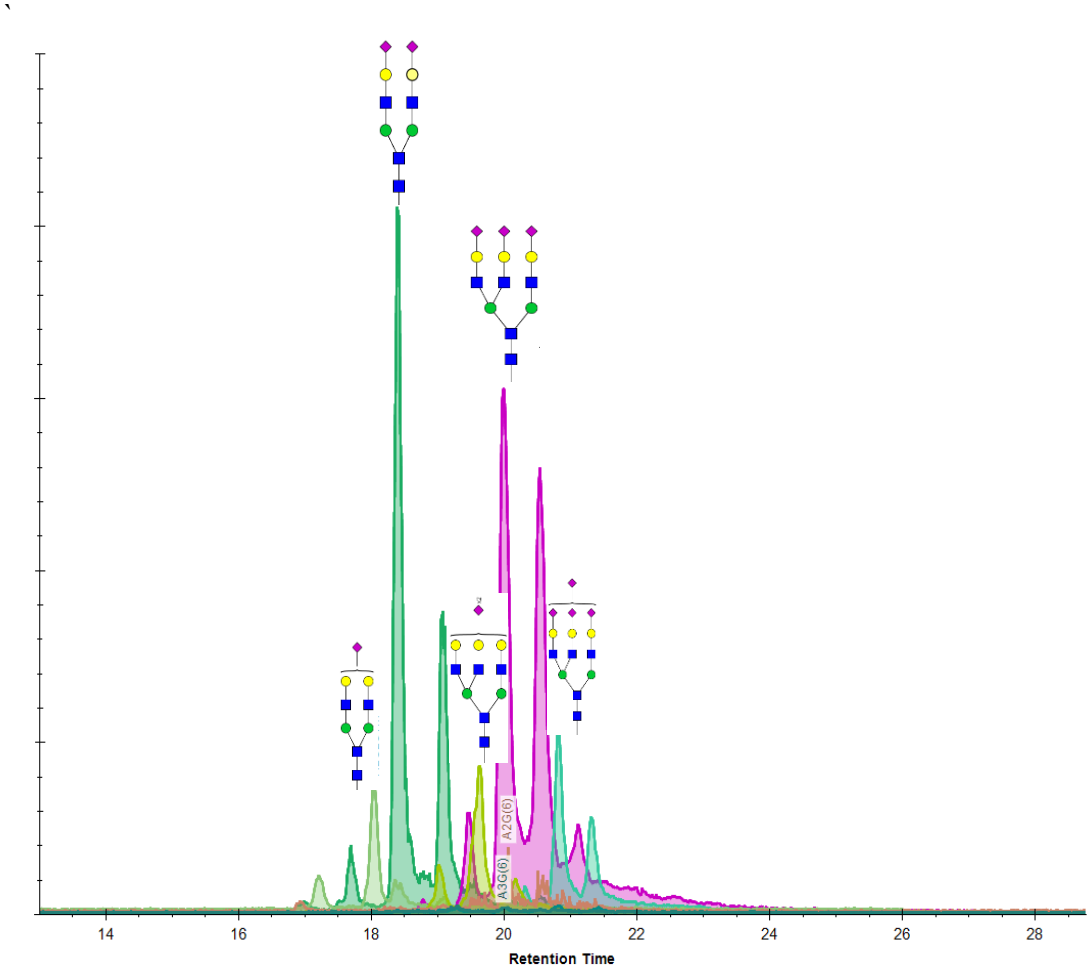

Figure 4.2 Chromatographic separation of fetuin-derived N-glycans on the negatively charged ZIC-HILIC stationary phase.

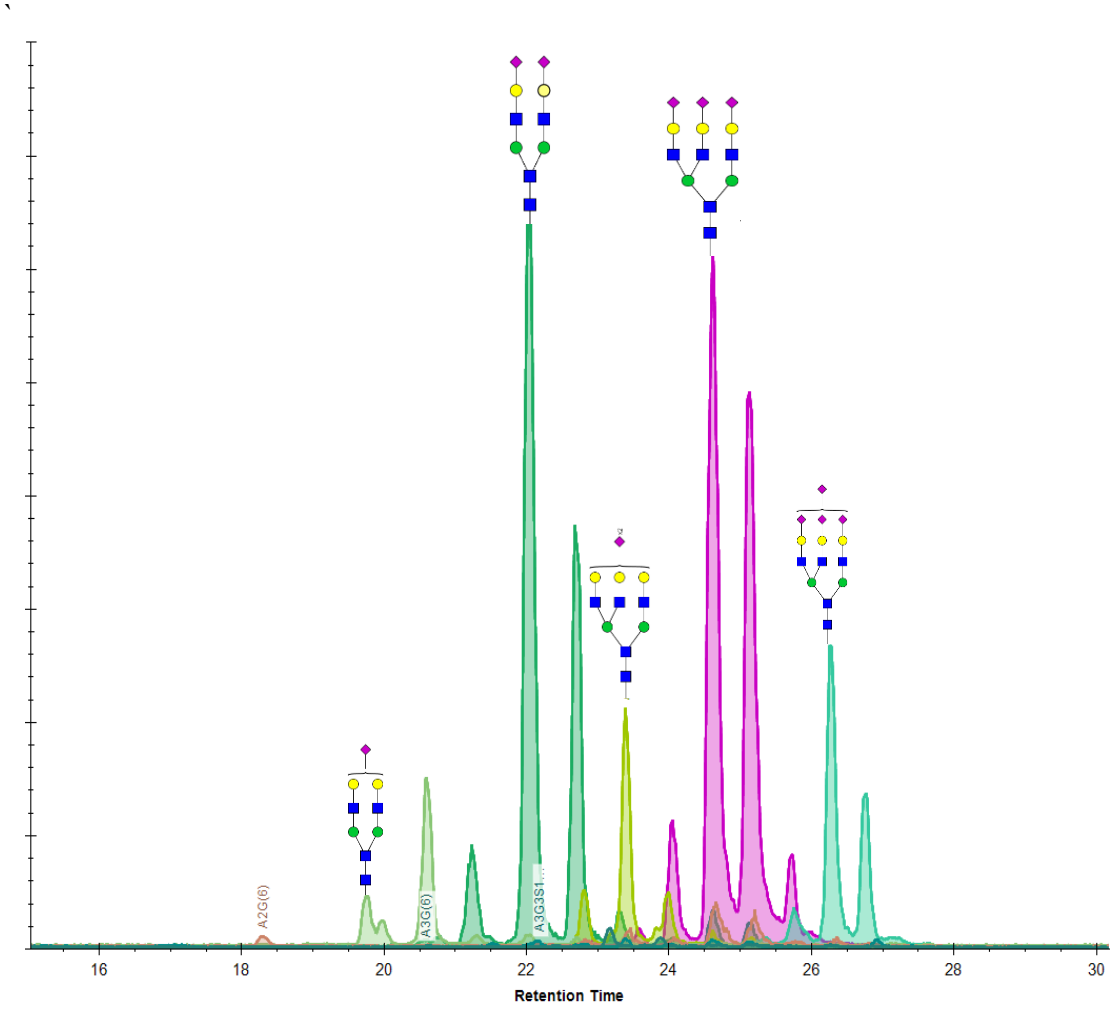

Figure 4.3 Chromatographic separation of fetuin-derived N-glycans on the positively charged ZIC-cHILIC stationary phase.

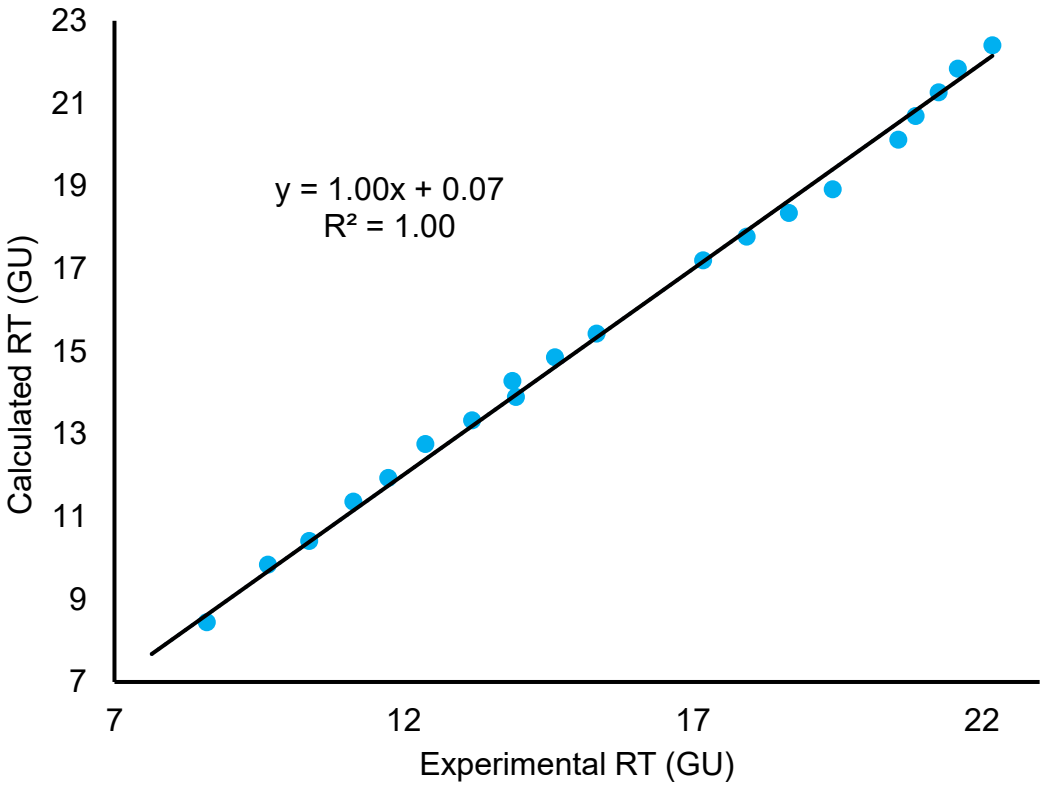

Figure 4.4 Evaluation of the Penta-HILIC retention model on the neutral column.

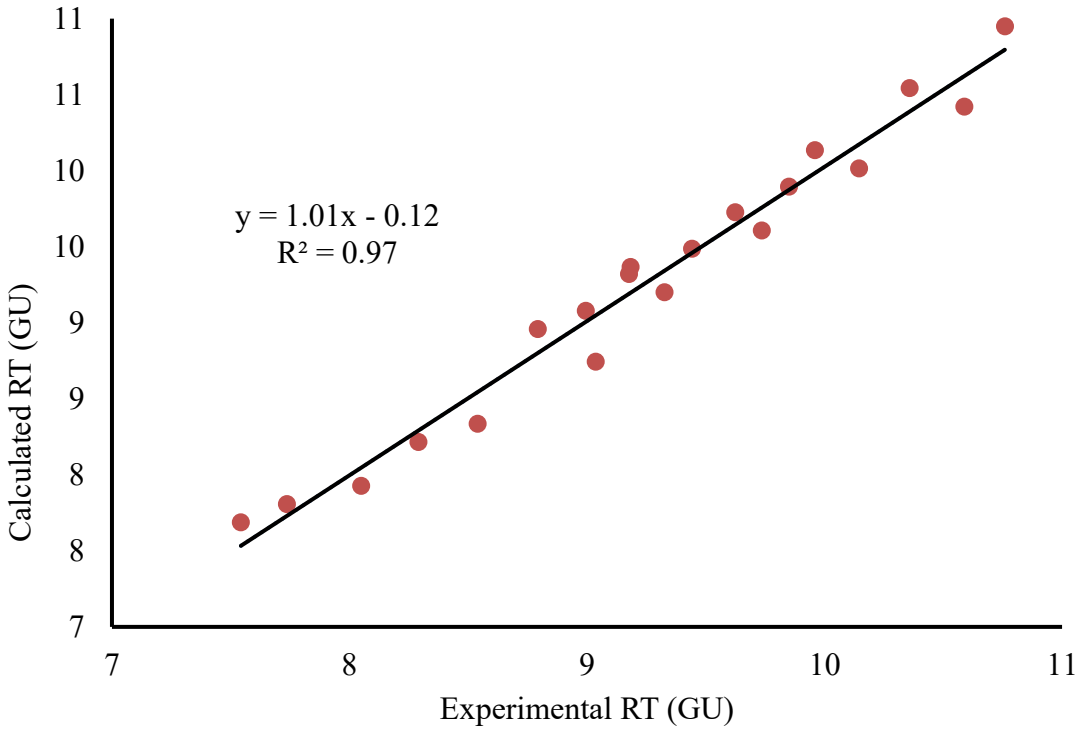

Figure 4.5 Retention time predictions on the negatively charged ZIC-HILIC column.

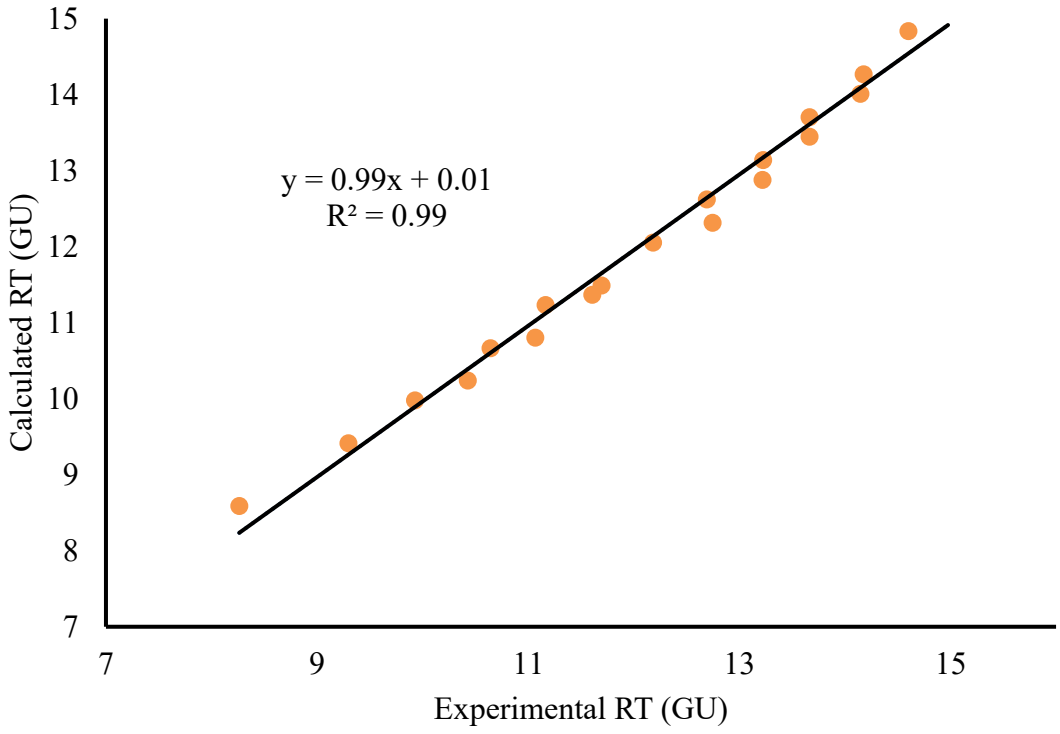

Figure 4.6 Retention time predictions on the positively charged ZIC-cHILIC column.

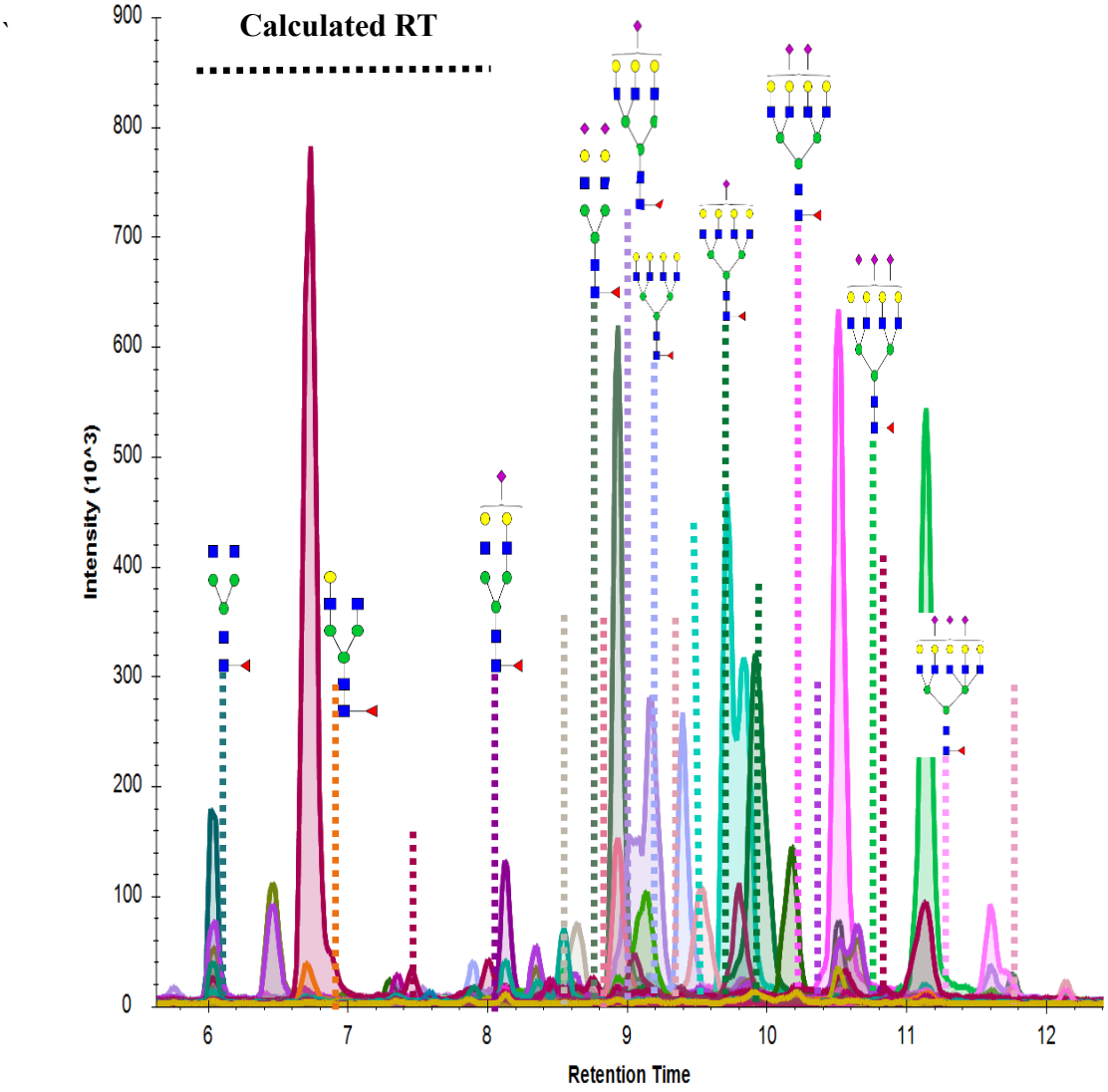

Figure 4.7 Chromatographic separation of epo-fc-derived N-glycans on the positively charged ZIC-cHILIC stationary phase.

Retention Motif	Penta-HILIC Coefficients	Zic-HILIC Coefficients	Zic-cHILIC Coefficients
GlcNAc	0.76	0.55	0.53
Man	0.67	0.70	0.85
Gal	0.82	0.60	0.72
SA (3)	2.92	0.12	0.82
SA (6)	3.49	0.53	1.39
Fuc core	1.06	0.29	0.36
Tag (ProA)	2.34	2.20	2.48
Tag (2-AA)	0.30	-	-
Tag (2-AB)	0.29	-	-

Table 4.1: Coefficients determined for each monosaccharide's retention contribution in the predictive HILIC retention model

References

1. Ajit Varki, & Harbor, S. (**2022**). *Essentials of Glycobiology*. Cold Spring Harbor Laboratory Press.
2. Alley, W. R., Mann, B. F., & Novotny, M. V. (2013). High-sensitivity Analytical Approaches for the Structural Characterization of Glycoproteins. *Chemical Reviews*, *113*(4), 2668–2732.
3. An, H. J., Froehlich, J. W., & Lebrilla, C. B. (**2009**). Determination of glycosylation sites and site-specific heterogeneity in glycoproteins. *Current Opinion in Chemical Biology*, *13*(4), 421–426.
4. Badgett, M. J., Mize, E., Fletcher, T., Boyes, B., & Orlando, R. (2018). Predicting the HILIC Retention Behavior of the N-Linked Glycopeptides Produced by Trypsin Digestion of Immunoglobulin Gs (IgGs). *Journal of Biomolecular Techniques JBT*, *29*(4), 98–104.
5. Cao, L., Qu, Y., Zhang, Z., Wang, Z., Iya Prytkova, & Wu, S. (**2016**). Intact glycopeptide characterization using mass spectrometry. *Expert Review of Proteomics*, *13*(5), 513–522.
6. Chongsaritsinsuk, J., Rangel-Angarita, V., Lucas, T. M., Mahoney, K. E., Enny, O. M., Mitchelle Katemauswa, & Malaker, S. A. (2024). Quantification and Site-Specific Analysis of Co-occupied N- and O-Glycopeptides. *Journal of Proteome Research*.

7. Chu, C. S., Niñonuevo, M. R., Clowers, B. H., Perkins, P. D., Hyun Joo An, Yin, H., Killeen, K., Miyamoto, S., Grimm, R., & Lebrilla, C. B. (2009). Profile of native ***N***-linked glycan structures from human serum using high performance liquid chromatography on a microfluidic chip and time-of-flight mass spectrometry. *Proteomics*, *9*(7), 1939–1951.
8. Dutta, D., Mandal, C., & Mandal, C. (**2017**). Unusual glycosylation of proteins: Beyond the universal sequon and other amino acids. *Biochimica et Biophysica Acta (BBA) - General Subjects*, *1861*(12), 3096–3108.
9. Han, L., & Costello, C. E. (**2013**). Mass spectrometry of glycans. *Biochemistry (Moscow)*, *78*(7), 710–720.
10. Hao, C., Zou, Q., Bai, X., & Shi, W. (2025). Effect of glycosylation on protein folding: From biological roles to chemical protein synthesis. *IScience*, *28*(6), 112605.
11. He, M., Zhou, X., & Wang, X. (**2024**). Glycosylation: mechanisms, biological functions and clinical implications. *Signal Transduction and Targeted Therapy*, *9*(1).
12. Huang, Y., Nie, Y., Boyes, B., & Orlando, R. (2016). Resolving Isomeric Glycopeptide Glycoforms with Hydrophilic Interaction Chromatography (HILIC). *Journal of Biomolecular Techniques : JBT*, *27*(3), 98–104.
13. Kozak, R. P., Concepcion Badia Tortosa, Fernandes, D. L., & Daniel. (2015). Comparison of procainamide and 2-aminobenzamide labeling for profiling and identification of glycans by liquid chromatography with fluorescence detection coupled to electrospray ionization–mass spectrometry. *Analytical Biochemistry*, *486*, 38–40.

14. Leymarie, N., & Zaia, J. (2012). Effective Use of Mass Spectrometry for Glycan and Glycopeptide Structural Analysis. *Analytical Chemistry*, *84*(7), 3040–3048.

15. LIS, H., & SHARON, N. (**1993**). Protein glycosylation. Structural and functional aspects. *European Journal of Biochemistry*, *218*(1), 1–27.

16. Mize, E. M. (2017). *Novel HILIC-MS Strategies for Retention Prediction and Quantitative Analysis of Glycomic and Glycoproteomic Analytes*.

17. Mulloy , B., Hart , G., & Stanley P, S. (**2009**). *Essentials of glycobiology*. Cold Spring Harbor Laboratory Press, Cop.

18. Pabst, M., Kolarich, D., Pöltl, G., Dalik, T., Lubec, G., Hofinger, A., & Altmann, F. (2009). Comparison of fluorescent labels for oligosaccharides and introduction of a new postlabeling purification method. *Analytical Biochemistry*, *384*(2), 263–273.

19. Planinc, A., Bones, J., Dejaegher, B., Van Antwerpen, P., & Delporte, C. (2016). Glycan characterization of biopharmaceuticals: Updates and perspectives. *Analytica Chimica Acta*, *921*, 13–27

20. Ruhaak, L. R., Zauner, G., Huhn, C., Bruggink, C., Deelder, A. M., & Wuhrer, M. (**2010**). Glycan labeling strategies and their use in identification and quantification. *Analytical and Bioanalytical Chemistry*, *397*(8), 3457–3481

21. Santos, A. L., & Lindner, A. B. (**2017**). Protein Posttranslational Modifications: Roles in Aging and Age-Related Disease. *Oxidative Medicine and Cellular Longevity*, *2017*, 1–19.

22. Shaw, C. J., Chao, H., & Xiao, B. (2001). Determination of sialic acids by liquid chromatography–mass spectrometry. *Journal of Chromatography A*, *913*(1-2), 365–370.

23. Smith, J., Millán-Martín, S., Mittermayr, S., Hilborne, V., Davey, G., Polom, K., … Bones, J. (2021). 2-Dimensional ultra-high performance liquid chromatography and DMT-MM derivatization paired with tandem mass spectrometry for comprehensive serum N-glycome characterization. *Analytica Chimica Acta*, *1179*, 338840–338840.
24. Zhou, Q., & Qiu, H. (2019). The Mechanistic Impact of N-Glycosylation on Stability, Pharmacokinetics, and Immunogenicity of Therapeutic Proteins. *Journal of Pharmaceutical Sciences*, *108*(4), 1366–1377.

CHAPTER 5

EVALUTING THE MASS TRANSFER MECHANISM OF HILIC SEPARATIONS

4 Brown, M., Orlando, R. To be submitted to a peer-reviewed journal

Abstract

Hydrophilic interaction liquid chromatography (HILIC) provides an alternative approach to effectively separate small polar compounds on polar stationary phases which are useful for many applications[4]. However, when optimizing the separation, little thought is explored in the method development area compared to reversed-phase liquid chromatography (RPLC). Most method development work is focused on the modification of the stationary phase and mobile phases, but little work has been explored on how the analyte diffuses in and out of the particle. In this study, the effect of pore size on mass transfer resistance is evaluated by comparing column performance using HILIC stationary phases with varied pore sizes. Van Deemter analysis was used to assess column efficiency across a range of flow rates.

Keywords: Hydrophilic Interaction Liquid Chromatography (HILIC), Method Development

Introduction

Hydrophilic interaction chromatography (HILIC) is a useful tool for separating hydrophilic analytes, which are challenging to resolve by reverse-phase LC (RP-LC).[1,13] Various methods have been explored for improving chromatographic performance such as exploring selectivity and optimizing mobile phase, and separation conditions.[3,10,17] While optimizing separations have been widely studied, the influence of mass transfer on HILIC performance has received relatively little attention.[10]

Initially created by Dr. Andrew Alpert's hypothesis[1], HILIC primarily operates through partitioning of polar analytes within a water-enriched layer on the stationary phase. The primary retention mechanism is thought to involve the partitioning between the mobile phase and water rich stationary phase.[9] This statement suggest that improvement strategies for HILIC can be optimized mostly by modification of the HILIC stationary phase.

Although prior studies have focused on modification of the stationary phase to enhance the ability to retain polar analytes, the effects of optimizing pore size, analyte size, and particle type have yet to be explored in the literature for HILIC. In reverse phase (RP) chromatograph pore size significantly influences method performance due to its effects on analyte diffusion and surface interactions.[4,6] These properties are often evaluated using the van Deemter equation,[14] which relates column efficiency to parameters like analyte diffusion, eddy diffusion, and mass transfer.[7] Despite its relevance, similar evaluations in HILIC mode have been limited.

This study will investigate the impact of pore size and particle type on HILIC performance, with a focus on carbohydrate separations. Mass transfer resistance was

evaluated as a contributing factor to chromatographic performance using both fully porous particles (FPP) and superficially porous particles (SPP). To better understand the separation mechanisms, retention factor, resolution, and peak width were measured for standard carbohydrate analytes.

Methods

Sample Preparation

Dextran was suspended in 50mM Ammonium Bicarbonate (1ug/ul) and labeled via reductive amination with Procainamide (ProA). Labeling was performed with sodium cyanoborohydride (NaBH3CN). 60 µL of 0.4 M Procainamide HCl (Sigma Aldrich, St. Louis, MO, USA), 0.8 M NaBH3CN (Sigma Aldrich, St. Louis, MO, USA) was added to this part, mixed in dimethyl sulfoxide :acetic acid;7:3 (v/v) and incubated at 65°C overnight. All fluorophores followed this same procedure. Samples were then dried using speed vacuum. Then the sample was resuspended in 5% acetic acid (240µL) and cleaned on a PD MiniTrap G10 desalting column (Cytiva, Marlborough, MA, USA) using the manufacturer's protocol. The samples were then dried and resuspended in 100% Milli-Q water (1 mg/mL) for LC-MS analysis.

LC-MS Experiments

LC separations were performed on zwitterionic stationary phases. Separations were conducted using ZIC-HILIC columns (Millipore Sigma, Bellefonte, PA,USA). Experiments were conducted using the Nexera UFLC (Shimadzu, Kyoto, Kyoto, Japan) coupled with the Synapt G2Si Q-TOF (Waters, Milford, MA, USA). All experiments were interpreted with Skyline and MassLynx (Waters, Milford, MA, USA) software for spectrum interpretation. Three columns were used, 160Å SeQuant ZIC HILIC, 2.7µm

superficially porous- 150 x 2.1 mm, 90Å SeQuant ZIC HILIC, 2.7µm superficially porous- 150 x 2.1 mm, and 200Å SeQuant ZIC HILIC, 5µm fully porous- 150 x 2.1 mm. All LC separations were performed using gradient conditions at 80-40%B over 40 min at varied flow rates (varied flow rate (0.5µL – 1.0mL/min and column temperature of 60^{c}. Mobile phase A consisted of 50mM ammonium formate + 0.1 % Formic Acid at pH 4 and mobile phase B was acetonitrile + 0.1% Formic Acid at pH 3.

Chemicals and samples

Procainamide labeled dextran (Sigma Aldrich, St. Louis, MO, USA) was used to evaluate HILIC performance. Purity of monosaccharide standards were in the range 95–99%. Acetonitrile, water, and formic acid are HPLC grade and purchased from Fisher Scientific (Hampton, NH, USA).

Results/ Discussion

HILIC performance was evaluated by exploring the mass transfer effects of two zwitterionic HILIC columns with a 2.7µm particle, 2.1mm x 150 with 90 and 160Å pore size. The mechanism was further explored between zwitterionic HILIC fully porous particles (FPP) with 200Å pores and 5µm particles and 2.7µm superficially porous particles (SPP) were evaluated. The role of mass transfer resistance in influencing chromatographic efficiency was explored also. Results will describe evaluation of retention trends across stationary phases, as well as comparison of resolution and peak width as a function of pore size and particle type.

Evaluation of pore size performance

Evaluation of the effect of pore size on HILIC performance, peak capacity was measured across a range of flow rates (0.1 – 1.00 mL/min) for columns packed with

stationary phases of 90 Å, 160 Å, and 200 Å pore diameters (Figure 5.1). A carbohydrate polymer dextran with varying molecular weight of 400-3800 Dalton was used to explore this result. Peak capacity is defined[5] as the maximum number of peaks that can be theoretically separated on a column at given chromatographic conditions a resolution of at least one or more.

Peak capacity was measured by using the equation:

$$Pc = 1 + \frac{t_{R,last} - t_0}{w_{avgerage}}$$

$w_{average}$ = is the peak width at FWHM, $t_{R,last}$,= retention time of the last eluting analyte and t_0 = retention time of the first eluting analyte

The 160 and 90 Å pore size resulted in having the highest peak capacity. While the 200 Å pore size demonstrated the lowest peak capacities, with no significant increase at higher flow rates. As peak capacity is inversely related to peak width and related to efficiency[8] . The superficially porous particle column demonstrates that this relationship is true. SPP columns showed narrower peaks (smaller peak width) alluding to better column performance across different flow rates. This is suggesting that the water layer has a significant role in performance as all flow rates showed the same performance[16]. While the fully porous particles displayed lower peak capacity showing to be more affected by mass transfer resistance demonstrated by all flow rates. Across flow rate the peak capacity was not significantly different also confirming the water layer mechanism theory suggested by Andy Alpert[1]. This also gives insight into HPLC system performance by higher backpressure on the FPP vs the SPP[2]. These results highlight the role of particle type and pore size optimization in HILIC column design, especially for

complex analytes such as carbohydrates, which often require both high resolution and minimal band broadening.

Effects of resolution on different pore sizes

To further investigate the impact of pore size on separation performance, average resolution values were calculated as the difference in retention times divided by the average peak width plotted against flow rate for columns with pore sizes of 90 Å, 160 Å, and 200 Å (Figure 5.2). The 160 Å SPP stationary phase consistently delivered the highest average resolution. The 90 Å phase followed closely behind exhibiting a slight decline at higher flow rates which was not significantly significant. The FPP 200 Å phase showed the lowest resolution overall which was similar to peak capacity.

These observations are similar to a Deemter equation , which models the relationship between linear velocity and column efficiency. At lower flow rates, resolution is generally enhanced due to reduced mass transfer resistance (the C-term) [15]. However, as flow increases, analytes have less time to equilibrate between the mobile and stationary phases, and the resolution can plateau or decline. The superior performance of the SPP 160 Å phase suggests it minimizes the C-term by offering an optimal pore size which allows sufficient analyte accessibility while maintaining efficient mass transfer. The 90 Å phase, although initially competitive, may restrict diffusion into smaller pores at higher velocities, slightly diminishing resolution. In contrast, the broader pores of the FPP 200 Å phase may reduce surface area which contribute to reduced interaction and broader peaks. Together with the peak capacity results, these data demonstrate that pore size significantly affects chromatographic resolution under HILIC conditions. The 160 Å material appears to offer the best balance of surface area,

accessibility, and diffusion kinetics for carbohydrate separations over a wide range of flow rates.

Band broadening effects

Band broadening in chromatography refers to how an analyte spreads out as it travel through the LC column. Wider peaks indicate a lower separation efficiency due to band broadening effects. Peak widths were calculated for small molecules were represented by looking at a dextran standard with vary mass ranges of 400-3600 Da. Glucose unit 4 and 20 were plotted as a function of linear velocity for both 90 Å and 160 Å pore size columns (Figure 5.3). Across all velocities, the 160 Å column generally produced narrower peaks for GU 4 which is a small molecule of 886 Dalton, particularly at higher velocities, where peak widths decreased to below 0.1 minutes. For GU 20 (3479 Dalton), which is significantly larger, peak broadening was more pronounced, especially at low velocities, with the 90 Å column yielding the broadest peaks (>0.3 min at ~2 mm/s). This suggests that GU 20 experiences restricted diffusion within the narrower pore network of the 90 Å phase, resulting in poor mass transfer and longer elution times.

Mass transfer resistance

Exploring the relationship between the analyte size and as a function of mass transfer resistant which is the C-term of the van Deemter equation Larger molecules like GU 20 have slower diffusion coefficients and are more sensitive to pore accessibility. At lower velocities, these effects dominate, leading to broader peaks. As velocity increases, reduced residence time limits diffusion inefficiency, causing peak widths to plateau. The 160 Å phase offers wider pores, enabling better analyte penetration and reduced stagnant

mobile phase volume, which enhances mass transfer for larger glycans. This is evident in its superior performance for both GU 4 and GU 20.

The data reinforce that pore size selection is critical for analyte size-dependent separations, particularly in HILIC where surface interactions dominate retention. The 160 Å stationary phase provides a more optimal pore environment for both small and large carbohydrates, resulting in narrower peaks and improved efficiency across a broader velocity range.

Conclusion

Optimizing HILIC stationary phases is critical for improving chromatographic performance. Columns packed with superficially porous particles (SPP) consistently delivered higher efficiency and are transferable for faster throughput applications due to reduced mass transfer resistance. This advantage is not observed in reverse-phase systems. While differences in performance between the 90 Å and 160 Å pore sizes were not statistically significant, subtle improvements with the 160 Å phase suggest that analyte size and diffusion characteristics may still influence separation outcomes. In contrast, fully porous particles (FPP) with 200 Å pores showed lower efficiency, likely due to decreased surface area and higher band broadening. These conclusions highlight the importance of carefully selecting both pore size and particle type when designing HILIC separations. These experiments support Dr. Andrew Alpert's hypothesis[1] that the water rich layer on the stationary phase plays a dominant role in retention and efficiency which outweighs the influence of internal pore accessibility.

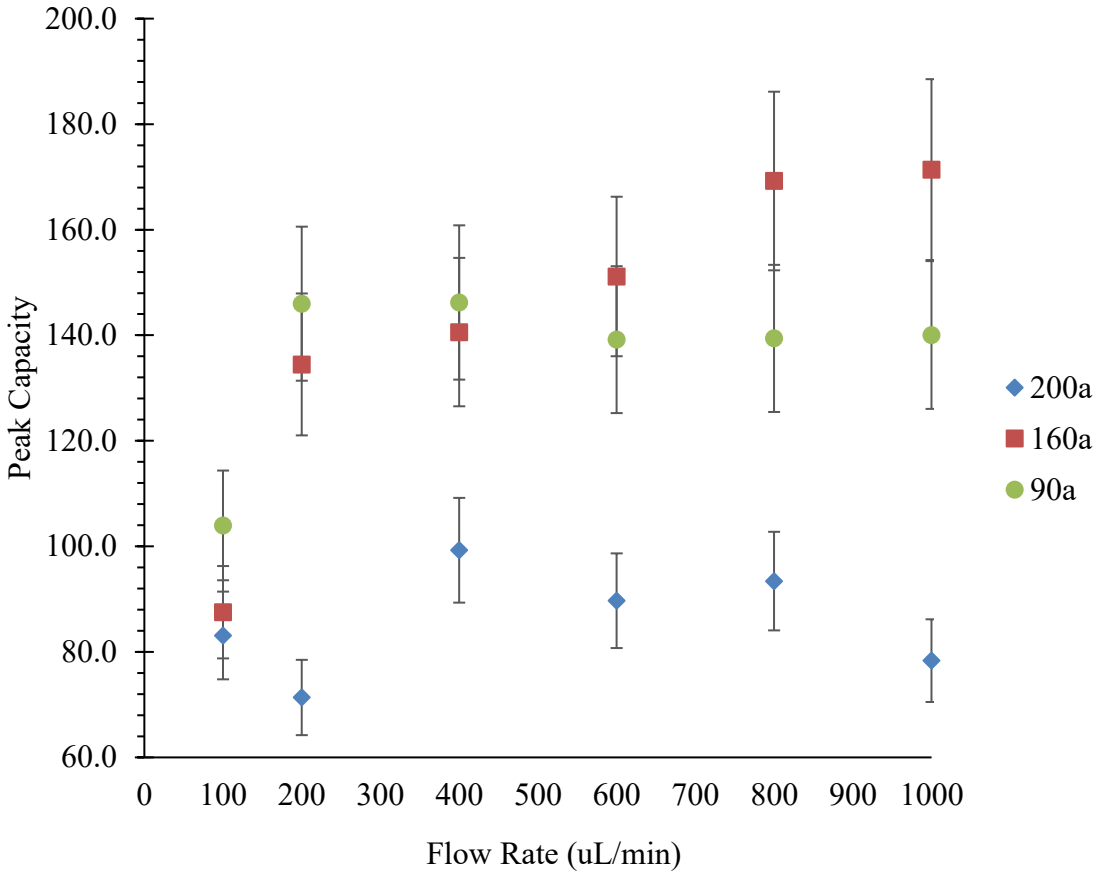

Figure 5.1 Peak capacity vs flow rate for three different stationary phases. The diamonds represent the fully porous (FPP) 200 Å pore size. The superficially porous particles are shown with the 90 Å (circle) and 160 Å (square).

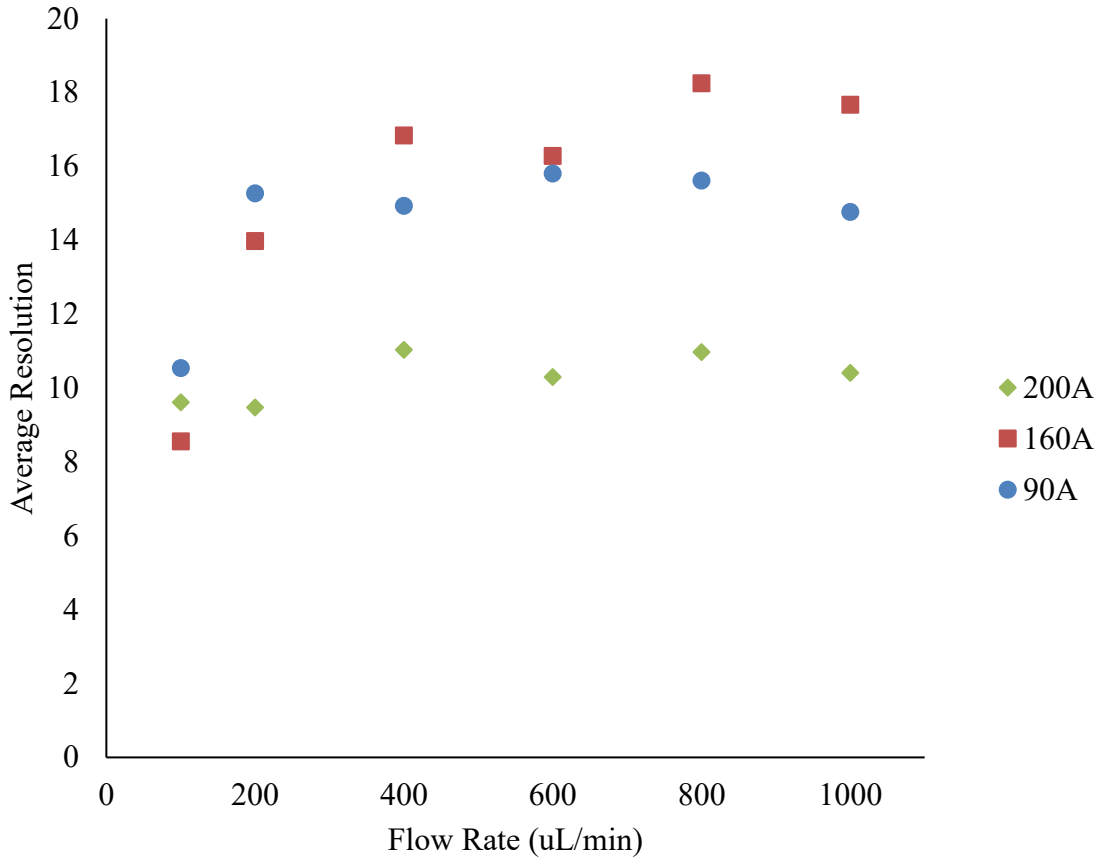

Figure 5.2 Average resolution vs flow rate. 90 Å (circle) and 160 Å (square) and 200 Å (diamond).

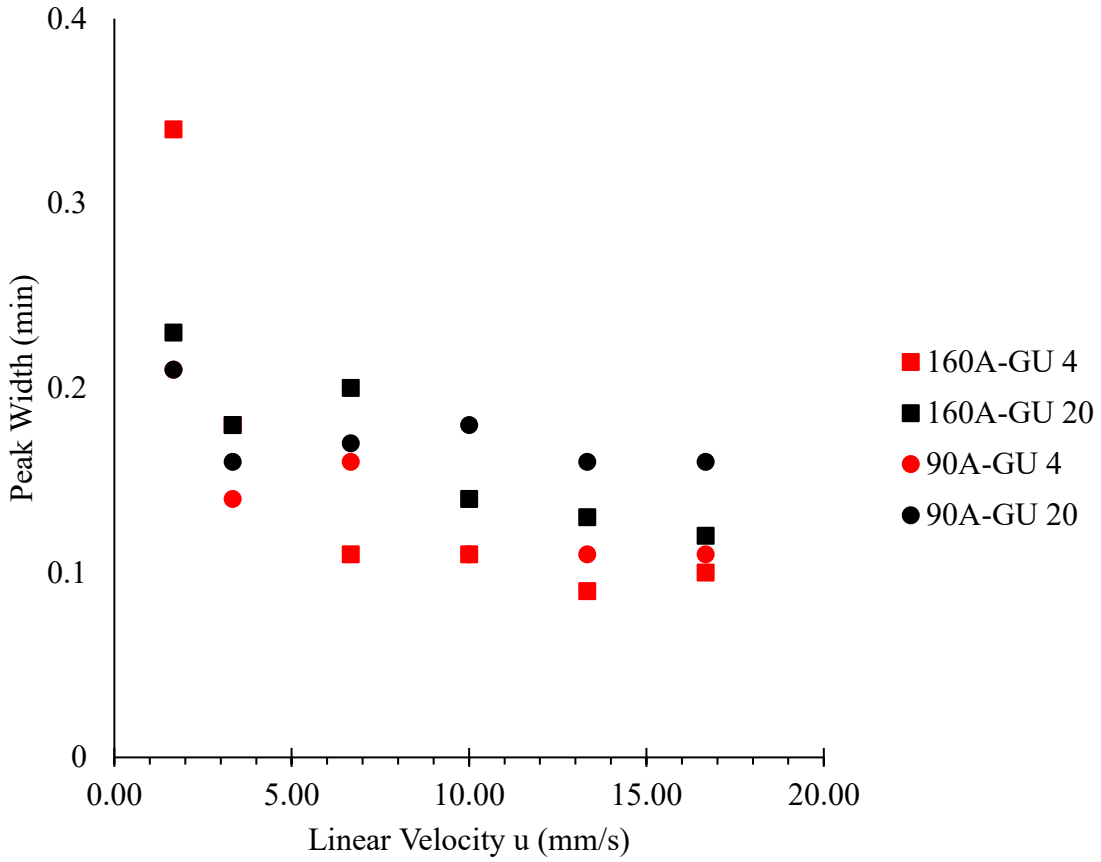

Figure 5.3 Effect of linear velocity vs. peak width for glucose units (GU) 4 (orange) and 20 (green) using zic-HILIC columns with 90 Å (circles) and 160 Å (square)pore sizes

References

1. Alpert, A. J. (1990). Hydrophilic-interaction chromatography for the separation of peptides, nucleic acids, and other polar compounds. *Journal of Chromatography A*, *499*, 177–196.
2. Bénédicte Chauve, Davy Guillarme, Philippe Cléon, & Jean-Luc Veuthey. (2010). Evaluation of various HILIC materials for the fast separation of polar compounds. *Journal of Separation Science*, *33*(6-7), 752–764.
3. Dejaegher, B., Mangelings, D., & Vander Heyden, Y. (2008). Method development for HILIC assays. *Journal of Separation Science*, *31*(9), 1438–1448.
4. Fausnaugh, J. L., Kennedy, L. A., & Regnier, F. E. (1984). Comparison of hydrophobic interaction and reversed-phase chromatography of proteins. *Journal of Chromatography A*, *317*, 141–155.
5. Gilar, M., Daly, A. E., Kele, M., Neue, U. D., & Gebler, J. C. (2004). Implications of column peak capacity on the separation of complex peptide mixtures in single- and two-dimensional high-performance liquid chromatography. *Journal of Chromatography A*, *1061*(2), 183–192.
6. Godinho, J. M., Naese, J. A., Toler, A. E., Boyes, B. E., Henry, R. A., DeStefano, J. J., & Grinias, J. P. (2020). Importance of Particle Pore Size in Determining Retention and Selectivity in Reversed Phase Liquid Chromatography. *Journal of Chromatography A*, *1634*, 461678.

7. Gritti, F., & Guiochon, G. (2015). The quantitative impact of the mesopore size on the mass transfer mechanism of the new 1.9 μm fully porous Titan-C18 particles II – Analysis of biomolecules. *Journal of Chromatography A*, *1392*, 10–19.
8. J.A. Navarro-Huerta, J.R. Torres-Lapasió, & M.C. García-Alvarez-Coque. (2018). Estimation of peak capacity based on peak simulation. *Journal of Chromatography A*, *1574*, 101–113.
9. Lídia Redón, Subirats, X., & Martí Rosés. (2020). HILIC characterization: Estimation of phase volumes and composition for a zwitterionic column. *Analytica Chimica Acta*, *1130*, 39–48.
10. McCalley, D. V. (2007). Is hydrophilic interaction chromatography with silica columns a viable alternative to reversed-phase liquid chromatography for the analysis of ionisable compounds? *Journal of Chromatography A*, *1171*(1-2), 46–55.
11. McCalley, D. V. (2010). Study of the selectivity, retention mechanisms and performance of alternative silica-based stationary phases for separation of ionised solutes in hydrophilic interaction chromatography. *Journal of Chromatography A*, *1217*(20), 3408–3417.
12. McCalley, D. V., & Neue, U. D. (2008). Estimation of the extent of the water-rich layer associated with the silica surface in hydrophilic interaction chromatography. *Journal of Chromatography A*, *1192*(2), 225–229.
13. McKeown, A. P. (2015). A simple, generally applicable HILIC method development platform based upon selectivity. *Chromatography Today, December*.

14. van Deemter, J. J., Zuiderweg, F. J., & Klinkenberg, A. (1956). Longitudinal diffusion and resistance to mass transfer as causes of nonideality in chromatography. *Chemical Engineering Science*, *5*(6), 271–289.
15. Wei, T.-C., Mack, A., Chen, W., Liu, J., Dittmann, M., Wang, X., & Barber, W. E. (2016). Synthesis, characterization, and evaluation of a superficially porous particle with unique, elongated pore channels normal to the surface. *Journal of Chromatography A/Journal of Chromatography*, *1440*, 55–65.
16. Wikberg, E., Sparrman, T., Viklund, C., Jonsson, T., & Irgum, K. (2011). A 2H nuclear magnetic resonance study of the state of water in neat silica and zwitterionic stationary phases and its influence on the chromatographic retention characteristics in hydrophilic interaction high-performance liquid chromatography. *Journal of Chromatography A*, *1218*(38), 6630–6638.
17. Wu, J., Bicker, W., & Lindner, W. (2008). Separation properties of novel and commercial polar stationary phases in hydrophilic interaction and reversed-phase liquid chromatography mode. *Journal of Separation Science*, *31*(9), 1492–1503.

CHAPTER 6

CONCLUSCIONS

This dissertation highlights how analytical strategies can be designed and refined to better resolve subtle structural differences in biomolecules—differences that often have profound biological implications. Through the use of ion mobility–mass spectrometry (IM-MS) and hydrophilic interaction liquid chromatography (HILIC), I was able to demonstrate how combining derivatization strategies with multidimensional separation techniques provides a powerful way to distinguish stereoisomers that are otherwise indistinguishable by conventional methods. The work began with monosaccharides. By derivatizing these sugars with optically pure amino acids, IM-MS separate D- and L-isomers but also probe how structural changes, particularly at stereocenters closer or farther from the derivatization site, affect gas-phase mobility. Tyrosine tagging stood out as a key strategy, giving consistent and meaningful separations across multiple isomeric classes. The same thinking was then applied in reverse using carbohydrates to tag amino acids. Here, maltotriose was found to be the most effective tag for separating enantiomeric amino acids in IM-MS, and this approach extended into peptide-level discrimination, allowing me to begin parsing out where in a peptide a D-residue might be present based on its mobility behavior.

As the work shifted toward glycans, the challenge became less about resolving enantiomers and more about modeling. HILIC retention times, when captured correctly,

can hold structural information. A predictive model was then used based on retention motifs that could work across different stationary phases, allowing for better interpretation even when MS alone couldn't give full resolution. The model worked well across neutral and zwitterionic columns and retained predictive accuracy even when the chromatographic conditions were varied.

Finally, the question of why HILIC behaves the way it does, especially when it comes to mass transfer resistance. Using dextran as a model pore size and particle type was evaluated for separation efficiency. The results backed up the hypothesis that the water-rich layer in HILIC plays a dominant role in retention and that mass transfer isn't just a reversed-phase problem. HILIC has its own unique considerations to improve performance.

Overall, this work offers a solution for challenging separations and contributes to a deeper mechanistic understanding of how stereoisomers and glycans behave in IM-MS and HILIC systems. There is still more to explore like improving resolution of larger peptides or testing alternative tags and drift gases. The experiments here creates a path forward for advancing separation science.